



## Review

## Non-thermal plasmas for non-catalytic and catalytic VOC abatement

Arne M. Vandenbroucke, Rino Morent\*, Nathalie De Geyter, Christophe Leys

Research Unit Plasma Technology, Department of Applied Physics, Faculty of Engineering, Ghent University, Jozef Plateastraat 22, 9000 Ghent, Belgium

## ARTICLE INFO

## Article history:

Received 27 February 2011

Received in revised form 19 August 2011

Accepted 22 August 2011

Available online 27 August 2011

## Keywords:

Non-thermal plasma

Plasma-catalysis

Volatile organic compounds

Waste gas treatment

## ABSTRACT

This paper reviews recent achievements and the current status of non-thermal plasma (NTP) technology for the abatement of volatile organic compounds (VOCs). Many reactor configurations have been developed to generate a NTP at atmospheric pressure. Therefore in this review article, the principles of generating NTPs are outlined. Further on, this paper is divided in two equally important parts: plasma-alone and plasma-catalytic systems. Combination of NTP with heterogeneous catalysis has attracted increased attention in order to overcome the weaknesses of plasma-alone systems. An overview is given of the present understanding of the mechanisms involved in plasma-catalytic processes. In both parts (plasma-alone systems and plasma-catalysis), literature on the abatement of VOCs is reviewed in close detail. Special attention is given to the influence of critical process parameters on the removal process.

© 2011 Elsevier B.V. All rights reserved.

## Contents

1. Introduction.....	30
2. Non-thermal plasmas for VOC abatement.....	31
2.1. Without catalyst.....	31
2.1.1. What is a non-thermal plasma?.....	31
2.1.2. Reactor concepts.....	31
2.1.3. VOC abatement.....	34
2.2. Combined with catalyst.....	38
2.2.1. What is plasma-catalysis?.....	38
2.2.2. Different types of catalysts.....	40
2.2.3. VOC abatement.....	40
3. Critical process parameters.....	47
3.1. Temperature.....	47
3.2. Initial VOC concentration.....	47
3.3. Humidity level.....	47
3.4. Oxygen content.....	48
3.5. Gas flow rate.....	48
4. Future trends.....	48
References.....	49

## 1. Introduction

Environmental protection is becoming an issue of growing concern in our globalized world. The industrialization of many economies has led to the emission of various kinds of substances that danger both human and ecological life [1]. Since World War II,

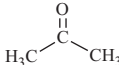
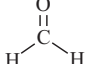
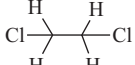
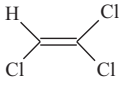
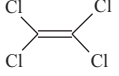


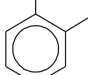
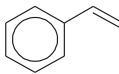
governments have become aware that emission legislation needs to become increasingly severe in order to ensure the protection of our environment for future generations. International treaties like the Kyoto protocol (1997) and the protocol of Gothenburg (1999) are important examples.

Exhausts from mobile (e.g. cars) and stationary sources (e.g. plants) pollute the air with a variety of harmful substances that threaten human and ecological life [2]. Next to NO<sub>x</sub>, SO<sub>x</sub>, H<sub>2</sub>S, . . . , volatile organic compounds (VOCs) are a large and important group of pollutants. Their high volatility causes them to rapidly

\* Corresponding author.

E-mail address: [Rino.Morent@UGent.be](mailto:Rino.Morent@UGent.be) (R. Morent).

**Table 1**  
Typical VOCs and their health effects.

VOC	Formula	Effects
Acetone		Carcinogen
Formaldehyde		Sore throat, dizziness, headache
Dichloroethane		Paralysis of nerve center
Trichloroethylene		Liver and kidney disease, paralysis of nerve center
Tetrachloroethylene		Probable heart and liver disease, skin irritation
Benzene		Carcinogen
Toluene		Headache, dizziness
Xylene		Headache, dizziness
Styrene		Probable carcinogen

evaporate and enter the earth's atmosphere. Depending on their chemical structure and concentration, they can cause various effects such as the creation of photochemical smog, secondary aerosols and tropospheric ozone [3]. They also have an effect on the intensification of global warming and on the deterioration of the stratospheric ozone layer. Some of them are toxic and cause odour nuisance while others have carcinogenic effects, proving their adverse effects on human health [4]. Table 1 provides an overview of typical VOCs that have been studied for removal with non-thermal plasma (NTP) and plasma-catalysis along with their related health effects.

Conventional methods to control VOC emissions are well-established technologies such as adsorption [5], thermal and catalytic oxidation [6], membrane separation [7], bioreaction [8] and photocatalysis [9]. The disadvantage of these methods is that they become cost-inefficient and difficult to operate when low concentrations of VOC need to be treated [10]. With the increased severity of emission limits in mind, this creates the need for an alternative technology that overcomes these weaknesses.

For the abatement of VOCs, NTP technology has attracted growing interest of scientists over the last 2 decades [11,12]. The energy that is delivered to the system, is almost completely consumed for accelerating electrons. They gain a typical temperature of 10,000–250,000 K (1–20 eV) [13], while the background gas remains at room temperature. This non-equilibrium state makes it unnecessary to heat the entire treated gas flow. Accelerated primary electrons collide with background molecules (N<sub>2</sub>, O<sub>2</sub>, H<sub>2</sub>O, . . .) producing secondary electrons, photons, ions and radicals. These latter species are responsible for the oxidation of VOC molecules, although ionic reactions are also possible. This process is highly

non-selective, creating a chemical reactive environment in which harmful substances are readily decomposed.

Although NTP for end-of-pipe application has been frequently proposed in literature for the removal of VOCs, NO<sub>x</sub> and SO<sub>2</sub>, . . . [14–16] formation of unwanted byproducts, poor energy efficiency and mineralization are serious roadblocks towards industrial implementation.

To overcome these problems, researchers are combining the advantages of NTP and catalysis in a technique called plasma-catalysis. This innovative method has become a hot topic over approximately the last ten years. The primary idea is that, by placing catalysts inside or in close vicinity of the discharge zone, retention time can be increased through adsorption of target molecules, favoring complete oxidation to CO<sub>2</sub> and H<sub>2</sub>O [17]. Interestingly, combining both techniques creates a synergism that is caused by various mechanisms [18–20].

This review gives an overview of the literature on plasma-assisted decomposition of VOCs with a special focus on plasma-catalysis. In the first part, an overview of different NTP reactors is given. In the second part, based on a large number of papers, an extended review is presented dealing with the treatment of VOCs with plasma-alone as well as with plasma-catalytic systems. Particular attention is paid to the most studied target compounds, i.e. trichloroethylene, benzene and toluene. Also general mechanisms that govern plasma-catalysis are summarized. In the third section, special attention is given to the influence of critical process parameters on the removal process. In the final section, future trends for this promising hybrid technique are discussed.

## 2. Non-thermal plasmas for VOC abatement

### 2.1. Without catalyst

#### 2.1.1. What is a non-thermal plasma?

Non-thermal plasmas are generated by applying a sufficiently strong electric field to ensure the discharge of a neutral gas. This creates a quasi neutral environment containing neutrals, ions, radicals, electrons and UV photons. Due to their light mass, electrons are selectively accelerated by the field and gain high temperatures while the heavier ions remain relatively cold through energy exchange by collisions with the background gas.

The bulk gas molecules (e.g. N<sub>2</sub>, O<sub>2</sub>) are bombarded by the electrons, typically having temperatures ranging from 10,000 K to 250,000 K (1–20 eV). This produces excited gas molecules (N<sub>2</sub><sup>\*</sup>, O<sub>2</sub><sup>\*</sup>) which lose their excess energy by emitting photons or heat. Next to excitation, other processes like ionization, dissociation and electron attachment occur in the discharge zone. Through these reaction channels, unstable reactive species like ions and free radicals are formed. Free radicals, such as OH<sup>\*</sup> and O<sup>\*</sup>, are highly reactive species which are ideal for the conversion of environmental pollutants to CO<sub>2</sub>, H<sub>2</sub>O and other degradation products at uncharacteristic low temperatures. The generation of NTP at atmospheric pressure and ambient temperature has been the subject of many research papers during the last two decades. This has led to great advances, mainly on laboratory scale. However, large-scale demonstrations of NTP technology for waste gas cleaning are also currently operative [13,21].

#### 2.1.2. Reactor concepts

Researchers have investigated a variety of NTP reactors for environmental purposes. The classification of these different reactors is rather complex and depends on multiple characteristics, such as:

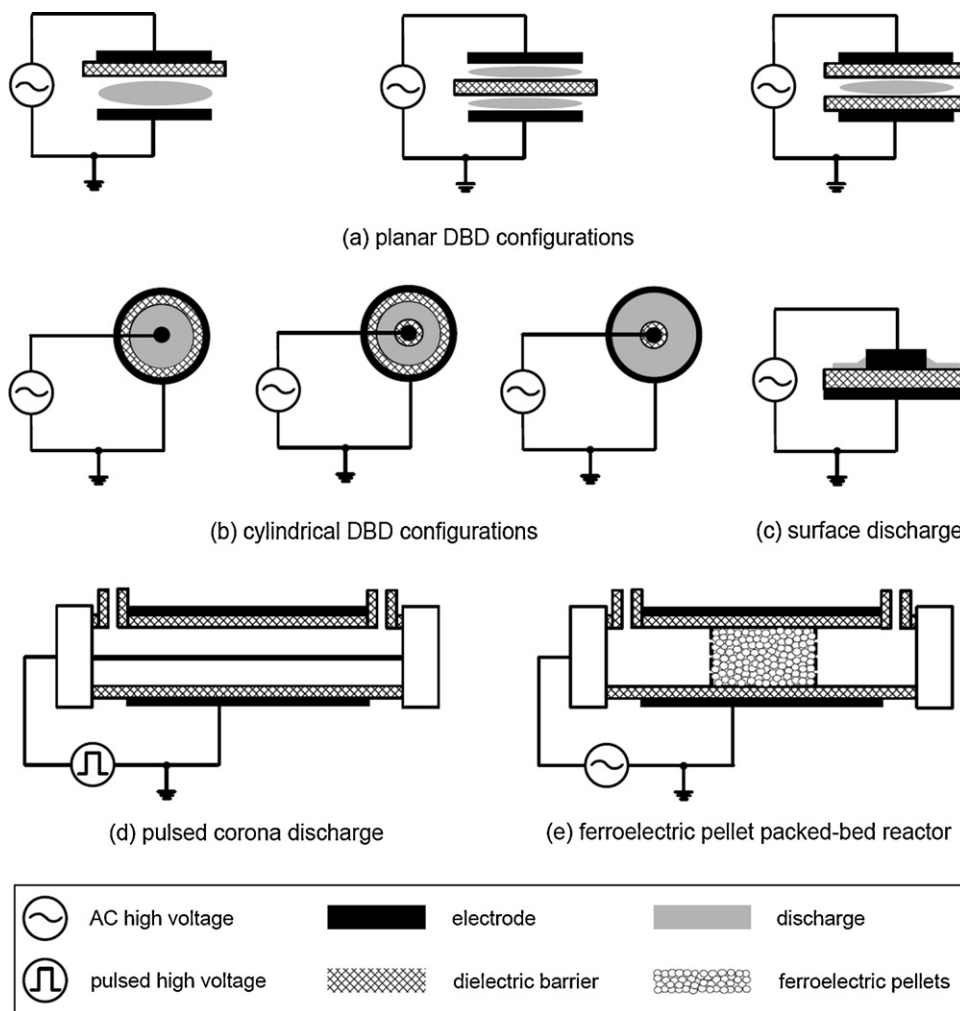


Fig. 1. Illustrations of various NTP reactor configurations.

- type of discharge: (DC or pulsed) corona discharge, surface discharge, dielectric barrier discharge, ferro-electric packed bed discharge,...
- type of power supply: AC, DC, pulse, microwave, RF,...
- other characteristics: electrode configuration, voltage level, polarity, gas composition,...

For the conventional NTP reactors that are employed in laboratory experiments, only the main characteristics will be briefly discussed here. A more detailed discussion can be found in literatures [22–27].

A *dielectric barrier discharge* (DBD) or silent discharge, typically has at least one dielectric (e.g. glass, quartz or ceramic) between the electrodes. DBDs are generally operated in one of the planar or cylindrical configurations shown in Fig. 1.

When the local electron density at certain locations in the discharge gap reaches a critical value, a large number of separate and short-lived current filaments are formed, also referred to as microdischarges. These bright, thin filaments are statistically distributed in space and time and are formed by channel streamers with nanosecond duration [28]. When a microdischarge reaches the dielectric, it spreads into a surface discharge and the accumulation of the transferred charge on the surface of the dielectric barrier reduces the electric field. As the electric field further reduces, electron attachment prevails over ionization and the microdischarges are extinguished. When the polarity of the AC voltage changes, the formation of a microdischarge is repeated at the same location if the

electron density again reaches a critical value necessary for electrical breakdown. Therefore, the use of the dielectric in the discharge zone has two functions: (1) limiting the charge transferred by an individual microdischarge, thereby preventing the transition to an arc discharge, and (2) spreading the microdischarge over the electrode surface which increases the probability of electron–molecule collisions with bulk gas molecules [28]. This type of arrangement is often referred to as a volume discharge [29].

Another type of arrangement to generate NTP in a DBD is the surface discharge [29] (Fig. 1(c)). Here for example, a series of strip electrodes are attached to the surface of a high-purity alumina ceramic base. A film like counter electrode is embedded in the inside of the alumina ceramic base and functions as an induction electrode. The ceramic can be either planar or cylindrical [30,31]. When an AC voltage is applied between the strip electrodes and the embedded counter electrode, a surface discharge starts from the peripheral edges of each discharge electrode and stretches out along the ceramic surface. The surface discharges actually consist of many nanosecond surface streamers. In another configuration to generate a surface discharge, strip electrodes can be placed on the inner surface of a cylindrical surface discharge reactor [32]. In this set-up, a DBD discharge is also formed between the central rod electrode and the surface electrodes.

A *pulsed corona discharge* (Fig. 1(d)) applies a pulsed power supply with a fast voltage rise time (tens of nanoseconds) to enable an increase in corona voltage and power without formation of sparks, which can damage the reactor and decrease the process efficiency.

The required voltage level to energize the discharge depends on the distance between the electrodes, the pulse duration and the gas composition [33]. The duration of a pulse voltage is typically in the order of 100–200 ns to ensure that spark formation is prevented and that the energy dissipation by ions is minimal. The latter is important to enhance the energy efficiency of the system. The electrode configuration of a pulsed corona discharge reactor can be either wire-to-cylinder [34–36] or wire-to-plate [37,38], although the former allows a better spatial distribution of the streamers and a higher energy density deposition in the gas [34]. The pulsed corona discharge usually consists of streamers, for which the ionization zone fills the entire electrode gap (e.g. 10 cm). This is favorable in terms of up-scaling and reducing the pressure drop. However, up-scaling is hampered by the high demands on the electronics of large pulsed power voltage sources.

A *ferroelectric pellet packed-bed reactor* (Fig. 1(e)) is a packed-bed reactor filled with perovskite oxide pellets. These reactors can have a parallel-plate or a coaxial configuration. Barium titanate (BaTiO<sub>3</sub>) is the most widely used ferroelectric material for environmental purposes, owing to its high dielectric constant ( $2000 < \epsilon < 10,000$ ). Other used ferroelectric materials are NaNO<sub>2</sub> [39], MgTiO<sub>4</sub>, CaTiO<sub>3</sub>, SrTiO<sub>3</sub>, PbTiO<sub>3</sub> [40] and PbZrO<sub>3</sub>–PbTiO<sub>3</sub> [41]. Application of an external electric field leads to polarization of the ferroelectric material and induces strong local electric fields at the contact points between the pellets and between the pellets and electrodes. This enables the production of partial discharges in the vicinity of each contact point between pellets. The presence of ferroelectric pellets in the discharge zone is beneficial for a uniform gas distribution and electrical discharge but causes an increase in pressure drop over the reactor length. Ferroelectric packed-bed reactors could serve as an alternative approach to enhance the energy efficiency, because the increase of the electric field will lead to a higher mean electron energy. Hence, the energetic electrons tend to form active species through dissociation and ionization, rather than forming less useful species through rotational and vibrational excitation. This leads to a more favorable consumption of the energy delivered, because electron-impact reactions are mainly

responsible for the plasma chemistry that destroys environmental pollutants.

A *DC corona discharge* is generated at atmospheric pressure when sharp points, edges or thin wires are subjected to a sufficiently large electric field. This causes a local increase of the electric field in the vicinity of the sharp curvature of the electrode. This is e.g. the case for a point-to-plate or for a wire-to-cylinder configuration. The corona discharge is initiated by acceleration of free electrons and subsequent electron collision processes. Due to formation of electron/positive-ion pairs and their separating process, an electron avalanche is created which sustains the corona discharge. Visually, this discharge is characterized by a weak glow region around the sharp electrode. Depending on the polarity of this electrode, the formation mechanism of the electron avalanche physically differs [22].

When the electrode with the strongest curvature is connected to the positive output of the power supply, a positive DC corona discharge is generated. Propagation of the discharge mainly depends on secondary photo-ionization processes around the sharp tip. The positive corona is characterized by the presence of streamers, i.e. numerous thin current filaments which are chaotically distributed in the gap. At a certain threshold voltage the discharge transitions from the stable corona mode to an unstable spark discharge regime.

In the case that the sharp electrode is connected to the negative output, a negative DC corona discharge is formed. Here, impact ionization of gas molecules is generally responsible for the propagation of the discharge. As the applied voltage increases, the negative corona will initially form Trichel pulse corona, followed by pulseless corona and spark discharge [22]. However, certain research groups [42–48] have succeeded in generating a glow discharge at atmospheric pressure before the negative corona shifts to a spark discharge. Akishev et al. [47] applied a special electrode geometry and a fast gas flow to stabilize the discharge, hence delaying it from creating sparks. Vertriest et al. [49] successfully tested the multipin-to-plate reactor concept for VOC abatement. Antao et al. [50] recently reviewed the operating regimes of atmospheric pressure DC corona discharges and their potential applications.

**Table 2**  
Overview of published papers on TCE removal with NTP.

Plasma type	Carrier gas	Flow rate (mL/min)	Concentration range (ppm)	Maximum removal efficiency (%)	Energy density (J/L)	Energy yield (g/kWh)	References
DBD	Ar/O <sub>2</sub>	10 <sup>4</sup>	500	>99	50	193.5 <sup>d</sup>	[51]
	Ar/O <sub>2</sub> /H <sub>2</sub> O			90	150	58 <sup>d</sup>	
DBD <sup>a</sup>	Air	700	250	>99	140	34.6 <sup>d</sup>	[115]
DBD <sup>b</sup>	Humid air	500	150–200	>99	480	8.1 <sup>d</sup>	[133]
DBD	Dry air	400	1000	95	150	122.5 <sup>d</sup>	[138]
			100	>99	135	14.3 <sup>d</sup>	
DBD	Dry air	400	100	99	200	9.6 <sup>d</sup>	[161]
DBD	Dry air	2000	250	98	120	39.5 <sup>d</sup>	[171]
DBD	Dry air	510	430	>99	350	23.8 <sup>d</sup>	[172]
DBD	Humid air	200–510	750	98–99	2400	6 <sup>d</sup>	[229]
DBD Surface discharge	Dry air	400	1000	99	1400	13.7 <sup>d</sup>	[143]
				95–99	1150	16.3 <sup>d</sup>	
DBD Pulsed corona	Dry air	2 × 10 <sup>4</sup>	160	85	100	26.3 <sup>d</sup>	[53]
				90	50	55.7 <sup>d</sup>	
Pulsed corona <sup>c</sup>	Humid air	–	1000	90	100	174.1 <sup>d</sup>	[52]
Pulsed corona	Dry air	–	100	80	50	30.9	[72]
Positive corona	Dry air	1500	100	67	580	2.2 <sup>d</sup>	[118]
DC negative glow discharge	Humid air	10 <sup>6</sup>	120	47	37	29.5 <sup>d</sup>	[49]
Capillary tube discharge	Dry air	1000	452	80	–	–	[78]

<sup>a</sup> Copper rod inner electrode.

<sup>b</sup> Inner electrode made of sintered metal fibres.

<sup>c</sup> Pulsed corona discharge with reticulated vitreous carbon electrodes.

<sup>d</sup> Calculated from data retrieved from reference.

**Table 3**  
Overview of published papers on benzene removal with NTP.

Plasma type	Carrier gas	Flow rate (mL/min)	Concentration range (ppm)	Maximum removal efficiency (%)	Energy density (J/L)	Energy yield (g/kWh)	References
DBD	Air (0–90% RH)	500–2000	500–2700	>99.9	2000–3000	–	[69]
DBD	Dry air	200	100	90	680	1.5 <sup>d</sup>	[70]
DBD	Humid air	10 <sup>4</sup>	276	>99	810	3.9 <sup>d</sup>	[71]
DBD	Dry air (5% O <sub>2</sub> )	4000–5000	200	75	305	5.7 <sup>d</sup>	[75]
DBD	Ar/2–40% O <sub>2</sub>	275	500–10 <sup>4</sup>	30	–	–	[77]
DBD	Dry air	250	300–380	11	170	2.5	[108]
DBD	Dry air	500	105	35	360	1.2 <sup>d</sup>	[129]
DBD	Dry air	400	200	70	3150	0.5 <sup>d</sup>	[163]
DBD	Dry air	4000	203–210	40	370	2.6 <sup>d</sup>	[175]
DBD	Dry air	1667	407	50	–	–	[179]
DBD	Dry air	35 × 10 <sup>3</sup>	250	50	230	6.3 <sup>d</sup>	[230]
Pulsed corona	Dry air	100	300	75	30	86.1 <sup>d</sup>	[90]
Positive DC corona <sup>a</sup>	Dry air	–	300	>99	–	–	[73]
DC glow <sup>b</sup>	Dry air	100	296	90	4000	0.9 <sup>d</sup>	[72]
BaTiO <sub>3</sub> packed-bed	Dry air	200	200	>99	3000	0.8 <sup>d</sup>	[40]
BaTiO <sub>3</sub> packed-bed	Humid air (0.5% H <sub>2</sub> O)	200	200	75	1800	1 <sup>d</sup>	[163]
BaTiO <sub>3</sub> packed-bed	Dry air	203–210	200	65	400	3.7 <sup>d</sup>	[174]
BaTiO <sub>3</sub> packed-bed	Dry air	–	110	98	130	9.4 <sup>d</sup>	[176]
BaTiO <sub>3</sub> packed-bed	Dry air	200	200	60	600	2.3 <sup>d</sup>	[212]
BaTiO <sub>3</sub> packed-bed <sup>c</sup>	Humid air (0.5% H <sub>2</sub> O)	200	200	95	1600	1.4 <sup>d</sup>	[231]

<sup>a</sup> Corona reactor is sealed after addition of benzene/air mixture.

<sup>b</sup> Microhollow cathode.

<sup>c</sup> Glass layer between two concentric electrodes.

<sup>d</sup> Calculated from data retrieved from reference.

### 2.1.3. VOC abatement

Tables 2–5 give an overview of published papers on VOC removal with NTP. For each reference, experimental conditions are given, along with the maximum removal efficiency and the corresponding energy yield in g/kWh calculated as followed:

$$\text{Energy yield} = \frac{C_{\text{in}} \times \eta \times M \times 0.15}{\varepsilon}$$

where  $C_{\text{in}}$  is the initial concentration (ppm) of the VOC with molecular weight  $M$  (g/mol),  $\eta$  the maximum removal efficiency and  $\varepsilon$  the corresponding energy density (J/L), i.e. the energy deposited per unit volume of process gas. Each calculation is based on the fact that one mole of a gas occupies 24.04 L volume at standard ambient temperature and pressure (293 K and 101325 Pa).

In what follows, particular attention is paid to the most studied target compounds, i.e. trichloroethylene, benzene and toluene. In

Table 5, a selection has been made of other relevant, but less frequently studied VOCs. For more details about operating conditions and results, the reader can consult the corresponding references.

**2.1.3.1. Trichloroethylene.** As can be seen from Table 2, TCE is a chlorinated olefin which has attracted a lot of attention because it can be relatively easy removed by NTP without the addition of considerable energy. This results from the fact that reactive radicals, produced in the plasma discharge, easily add to the carbon-carbon double bond thereby initiating the oxidation process.

Evans et al. [51] carried out an experimental and computational study of the plasma remediation of TCE in dry and wet Ar/O<sub>2</sub> mixtures using a silent discharge plasma. They found that the ClO radical is an important intermediate which oxidizes TCE. In wet mixtures, ClO is partially consumed by OH radicals, resulting in a lower decomposition rate of TCE. They suggest a diagram

**Table 4**  
Overview of published papers on toluene removal with NTP.

Plasma type	Carrier gas	Flow rate (mL/min)	Concentration range (ppm)	Maximum removal efficiency (%)	Energy density (J/L)	Energy yield (g/kWh)	References
DBD	Dry air (5% O <sub>2</sub> )	4000–5000	200	75	310	6.6 <sup>b</sup>	[75]
DBD	N <sub>2</sub> dry air	2000	400	21	240	4.7 <sup>b</sup>	[81]
				23		5.2 <sup>b</sup>	
DBD	N <sub>2</sub> /5% O <sub>2</sub> (0.2% RH)	100	50	73	600	0.8 <sup>b</sup>	[82]
DBD	Humid air (55% RH)	1000	100	46	2100	0.3 <sup>b</sup>	[203]
DBD packed with glass pellets	Dry air	600	1100	75–80	1000	11.5 <sup>b</sup>	[167]
DBD packed with glass pellets	Humid air (95% RH)	500	500	91	18.5	11.5	[232]
DBD packed with glass beads	Dry air	315	240	36	172	6.8 <sup>b</sup>	[202]
Multicell DBD packed with glass beads <sup>a</sup>	Dry air	1000	110	72	2502	0.4 <sup>b</sup>	[224]
DC back corona	Dry air	100–750	5–200	93	2400	0.4 <sup>b</sup>	[79]
Pulsed corona	Dry air	450	500	>99	1000	6.7 <sup>b</sup>	[84]
Positive corona	Humid air (26% RH)	10 <sup>4</sup>	0.5	80	65	0.1 <sup>b</sup>	[83]
BaTiO <sub>3</sub> packed-bed	Dry air	–	101	95	125	–	[176]
Dielectric capillary plasma electrode discharge	Air	–	266.5	>99	3500	1 <sup>b</sup>	[233]
Capillary tube discharge	Dry air	350	1246	86	–	–	[78]

<sup>a</sup> Three cells.

<sup>b</sup> Calculated from data retrieved from reference.



**Table 5**

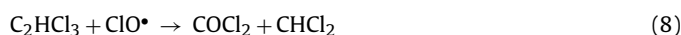
Published papers on removal of other VOCs with NTP.

Target compound	Reference
Acetaldehyde	[215,234]
Acetone	[31,235–240]
Acetylene	[241,242]
Dichloromethane	[210,235,243–246]
Formaldehyde	[191,194]
Methane	[72,218,219,247]
Methanol	[53,61,210,248–250]
Propane	[34,190,193,251–253]
Propene	[34,241,252,254,255]
Styrene	[256,257]
Tetrachloromethane	[61,216,235,245,258–260]
Xylene	[35,192,233,238,261]

of the dominant reaction pathways in plasma remediation of TCE giving CO, CO<sub>2</sub>, COCl<sub>2</sub> and HCl as main byproducts. According to the authors, the toxic byproduct phosgene (COCl<sub>2</sub>) can easily be removed from the exhaust stream by placing a water scrubber downstream of the plasma discharge. This is a cost effective post-treatment because removal of phosgene with their DBD reactor requires high energy. The authors propose the following reactions as the dominant degradation pathway for TCE in dry Ar/O<sub>2</sub> mixtures:



The ClO radical rapidly back-reacts with TCE leading to the formation of phosgene and methylchloride by the following reaction:

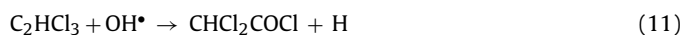
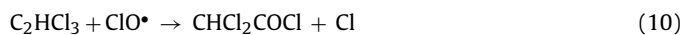


Methylchloride then quickly reacts with oxygen in the subsequent reaction:



In wet mixtures, two additional species can be produced by reaction of OH with TCE, CHCl<sub>2</sub>-COCl (dichloroacetylchloride; DCAC) and CHCl<sub>2</sub>.

DCAC is detected as main byproduct of TCE decomposition with a pulsed corona discharge by Kirkpatrick et al. They suggest the reaction of TCE with ClO radicals leading to the formation of DCAC under dry conditions, as follows [52]:



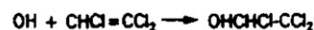
Under humid conditions the formation of DCAC is suppressed, suggesting that ClO radicals are quenched by OH radicals by the reaction:



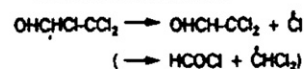
Cl radicals can further attack DCAC, leading to the formation of CO, HCl, CCl<sub>4</sub>, CHCl<sub>3</sub> and COCl<sub>2</sub> as final products.

The effect of temperature on the removal chemistry and byproduct formation of TCE is studied by Hsiao et al. [53]. Experiments, carried out with a pulsed corona and a DBD reactor, have shown that the removal of TCE and the formation of CO<sub>x</sub> depend on temperature but not on reactor type. Moreover, higher temperatures

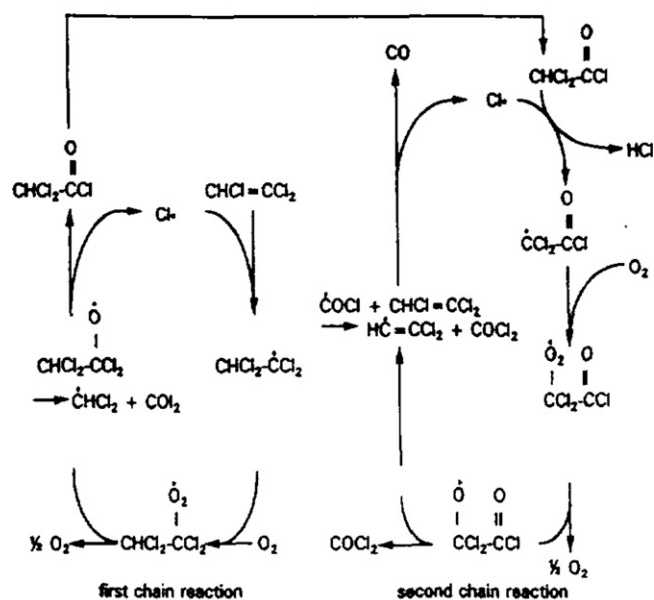
### Formation of OH radicals in electron-irradiated air



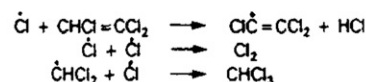
#### Chlorine radical formation



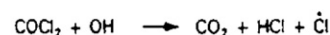
#### Chain reactions



#### Chain termination



#### Secondary reaction



#### Hydrolysis

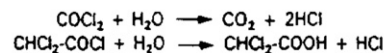


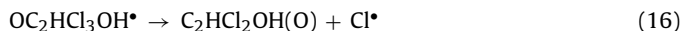
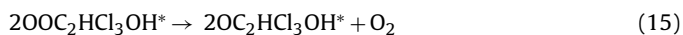
Fig. 2. TCE decomposition mechanism.

Reprinted from Ref. [54], with permission from Elsevier.

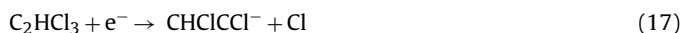
cause a decrease in energy yield for TCE. The formation of byproducts (CO, CO<sub>2</sub>, COCl<sub>2</sub>, HCl and DCAC) is almost the same as found by Evans et al. [51].

Prager et al. [54] report the degradation of TCE with electron beam treatment. They found CO, HCl, COCl<sub>2</sub>, DCAC and CHCl<sub>3</sub> as main byproducts next to traces of CCl<sub>4</sub> and CCl<sub>3</sub>-COCl (trichloroacetylchloride; TCAA). In the proposed degradation mechanism (Fig. 2), OH radicals add to the double bond of TCE forming OH adducts. These adducts decompose and produce chlorine radicals or to a minor extent dichloromethyl radicals. Next, chlorine radicals add to the double bond and in a subsequent reaction with oxygen, the corresponding peroxy radical is formed. In a bimolecular reaction step, molecular oxygen and alkoxy radicals are formed, which fragmentate to DCAC and chlorine which in turn re-enters the first chain reaction. In a second chain reaction, DCAC is further decomposed to HCl, COCl<sub>2</sub> and CO. To minimize the formation of chloroacetic acids and phosgene, a wet scrubbing system is installed downstream of the electron beam system. Hakoda et al.

[55,56] also conclude that TCE decomposition with electron beam proceeds via a Cl radical addition chain reaction induced by OH radicals via the following reactions:



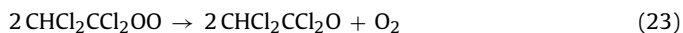
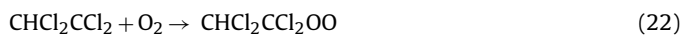
Vitale et al. [57] examined the effect of a carbon-carbon double bond on electron beam treatment of TCE. The primary decomposition products found in their study are CO, CO<sub>2</sub>, COCl<sub>2</sub>, DCAC and HCl. Chloroform and TCAA were found as minor decomposition products. These researchers propose a reaction pathway in which dissociative electron attachment is believed to be the primary initiation step. This reaction produces chlorine radicals and a doubly chlorinated ethylene anion:



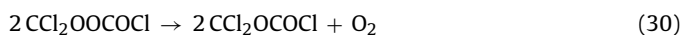
In a study by Yamamoto and Futamura [27], the pronounced decomposition of TCE in dry nitrogen also strongly argues for dissociative electron attachment as the first stage in the decomposition of TCE. Vitale et al. propose that the chlorinated ethylene anion will likely decompose by direct oxidation:



Then, in a secondary autocatalytic radical reaction, chlorine radicals add to the least substituted carbon atom of the double bond of TCE resulting in the start of a chlorine radical chain reaction [58,59]. Bertrand et al. [60] suggest that addition to the least chlorinated site is favored over addition at the more chlorinated site by at least a factor 8. A possible chlorine addition reaction mechanism for the favored reaction is as follows:



DCAC decomposes to form HCl, COCl<sub>2</sub> and chlorinated radicals through the following reaction:



Phosgene may further decompose through Cl abstraction by chlorine, oxygen or other radicals forming CO and Cl<sub>2</sub> or Cl radicals. The TCE removal rate is reduced by the presence of reaction products such as phosgene, HCl and DCAC through scavenging of electrons in the plasma which could otherwise initiate more dissociative electron attachment reactions of TCE.

The study of Penetrante et al. [61] shows that for small initial concentrations of TCE in dry air, the reaction with O radicals and

electrons seems to be the likely primary decomposition mechanism. These reactions initiate the detachment of Cl radicals, which in turn decompose more TCE molecules by Cl radical addition to the carbon-carbon double bond causing a chain reaction as proposed by Vitale et al. [57].

Futamura and Yamamoto [62] have applied a pulsed corona and a ferroelectric (BaTiO<sub>3</sub>) packed-bed reactor for TCE removal. In wet nitrogen, dichloromethane, chloroform, pentachloroethane, carbon tetrachloride, 1,1,2,2,- and 1,1,1,2-tetrachloroethanes and tetrachloroethylene are detected as major byproducts for the packed-bed reactor by using GC-MS (gas chromatography-mass spectrometry). Chloro- and dichloroacetylenes, (Z)- and (E)-1,2-dichloroethylenes, and 1,1,2-trichloroethane are obtained as minor byproducts. With a pulsed corona reactor, 1,1,2-trichloroethane is the main byproduct along with tetrachloroethylene, (Z)-1,2-dichloroethylene and negligible amounts of polychloromethanes. When air is used as carrier gas for the decomposition with the packed-bed reactor, only phosgene could be detected. For both reactors and for both carrier gases CO, CO<sub>2</sub>, NO<sub>x</sub> and N<sub>2</sub>O are also formed as byproducts. Formation of DCAC is, however, not observed in aerated conditions, which is in contrast with previous mentioned studies. The authors propose a plausible reaction mechanism under deaerated conditions. In the presence of O<sub>2</sub>, they suggest that triplet oxygen molecules scavenge intermediate carbon radicals derived from TCE decomposition in an autoxidation process. Unstable alkylperoxy radicals are generated and further oxidatively decompose to render CO and CO<sub>2</sub>, as shown in the following general reaction:



Urashima and Chang suggest that electron impact processes produce C, H, N radicals and negative ions. According to the authors the oxidation processes will take place directly by radicals or via oxidation of negative ions [63]. They propose a mechanism of TCE destruction based on 162 reactions [64].

In a study performed by Han and Oda [65], the effect of oxygen concentration on byproduct distribution is examined. TCE decomposition efficiency improves with decreasing oxygen content except for 0% oxygen. The formation of DCAC is maximal for 2% oxygen, while TCAA formation decreases with decreasing oxygen concentration. They suggest that oxygen species, like O(<sup>1</sup>D) or other states in the discharge, react more strongly with the precursor of DCAC (CHCl<sub>2</sub>-CCl<sub>2</sub>•) than that of TCAA (CCl<sub>3</sub>-CH•). When nitrogen is used as carrier gas, the GC-MS could detect HCl, Cl<sub>2</sub>, C<sub>2</sub>H<sub>2</sub>Cl<sub>2</sub>, CHCl<sub>3</sub>, CCl<sub>4</sub> and C<sub>2</sub>HCl<sub>5</sub> as byproducts. The authors suggest that collisions between TCE and electrons and (or) N<sub>2</sub> excited species (N<sub>2</sub><sup>\*</sup>) generate chlorine radicals. The main decomposition mechanism is considered to be the chlorine radical chain reaction as mentioned before by other authors.

**2.1.3.2. Benzene.** Benzene has attracted attention for NTP removal because it is a carcinogenic compound that has detrimental effects on human health. Table 3 summarizes published papers on benzene removal with NTP.

In order to minimize operation costs for NTP removal it is important to optimize the operation conditions. Ogata et al. [40] investigated the effects of properties of ferroelectric materials, AC frequency, initial concentration of benzene and the concentration of O<sub>2</sub> in the background gas for the removal of benzene in air using a ferroelectric packed-bed reactor. Under dry conditions benzene removal results in a low CO<sub>2</sub>-selectivity and in the formation of various byproducts, such as CO, C<sub>2</sub>H<sub>2</sub>, N<sub>2</sub>O, NO and NO<sub>2</sub>.

To improve this technique for practical applications, Ogata et al. [66] have studied the effect of water vapor on the removal of benzene with a ferroelectric packed-bed reactor. They suggest that a portion of the lattice oxygen species in BaTiO<sub>3</sub> pellets is deactivated

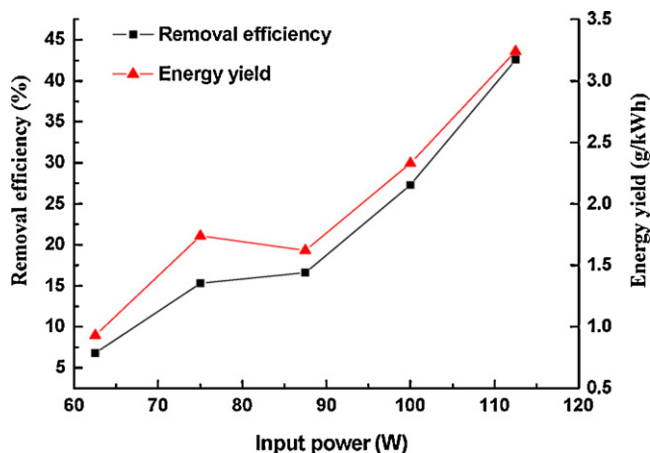


Fig. 3. Effect of input power on benzene removal efficiency and energy yield. Reprinted from Ref. [71], with permission from Elsevier.

by adsorption of  $H_2O$  on the surface of the pellets. This results in a suppressed formation of  $CO$  and  $N_2O$ , a higher  $CO_2$ -selectivity and a lower decomposition of benzene. These observations are confirmed by Kim et al. [67]. The negative effect of humidity on benzene removal is ascribed to the interaction of water vapor with the surface of  $BaTiO_3$  pellets which may alter the surface state. As a consequence, plasma properties may be negatively affected [68], resulting in slower chemical destruction pathways.

Cal and Schluep [69] investigated the decomposition of benzene in a DBD reactor as a function of the relative humidity (RH) without the presence of ferroelectric pellets. In both dry and wet gas streams, near complete destruction (>99.9%) of benzene is achieved and no intermediate hydrocarbons are observed with GC-MS. However, in wet gas streams the mineralization degree is greatly improved compared to dry air. Unfortunately, at high RH, a polymeric film is produced on the dielectric plates which slowly decreases the removal efficiency of benzene through time.

Lee et al. [70] also used a DBD discharge to decompose 100 ppm of benzene in air. The authors suggest a plausible reaction mechanism that includes the formation of all byproducts detected by GC-MS and FT-IR (Fourier transform-infrared) spectroscopy. According to the authors, the plasma can produce O radicals from  $O_2$ , which can react with benzene to form  $CO_2$ ,  $H_2O$  and benzene cation by a series of reactions. Benzene could directly be decomposed by the plasma to form phenol and benzenediol. The plasma is also capable of decomposing stable  $CO_2$  to form CO radicals that would add to phenol. This leads to the formation of secondary products such as benzaldehyde and benzoic acid. Finally, decomposition of  $H_2O$  by the discharge forms H and OH radicals which lead to the formation of benzene, phenol and benzenediol.

Also, Ye et al. [71] have investigated the feasibility of benzene destruction with a DBD discharge. Experiments are carried out with a laboratory scale and a scale-up DBD reactor. With the former reactor, high removal efficiencies are obtained with lower flow rates, lower initial concentrations and higher input power (Fig. 3). In contrast, higher initial concentration and input power provide a high-energy efficiency for benzene removal. For the scale-up reactor, adding DBD systems in series can enhance the decomposition efficiency to a large extent. However, after a certain treatment time brown polymeric deposits are formed on the inside wall of the reactor which can finally lead to mechanical failure of the dielectric due to thermal energy built up. The deposit can be removed by passing air through the reactor at 6 kV for several minutes. GC-MS analysis revealed that phenol, hydroquinone and nitrophenol are the main products contained in the deposition. The feasibility study shows that multiple DBD systems in series can enhance the removal

efficiency of benzene to a large extent and proves that DBD treatment is competitive with other technologies although formation of solid residues and aerosol particles are issues that must be solved to secure an effective operation.

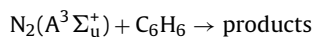
In a study by Jiang et al. [72], a DC microhollow cathode glow discharge is applied to remove 300 ppm benzene from dry air. The authors use a zero-dimensional plasma chemistry code (KINEMA) [73] to model the benzene dissociation mechanism in a benzene/dry air mixture plasma. Important dissociation reactions predicted by the model are:



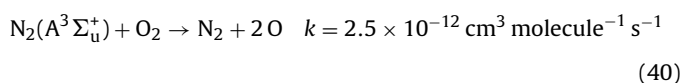
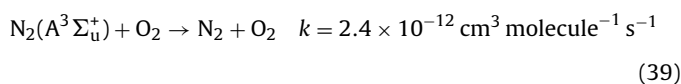
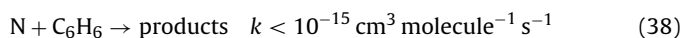
Modeling results reveal that the dominant dissociation reactions for benzene destruction in the DC glow discharge are atomic oxygen impact reactions. They suggest that the benzene destruction rate and efficiency are limited due to atomic oxygen losses in the boundary layer of the dielectric walls, which confine the discharge in the direction perpendicular to the gas flow direction.

Satoh et al. [73] have applied a positive DC corona discharge between a multi-needle and a plane electrode for the removal of 300 ppm benzene in different  $N_2/O_2$  mixtures. Analysis of the exhaust stream is performed with FT-IR and shows  $C_2H_2$ , HCN, NO and HCOOH as intermediate products and  $CO_2$  as an end product. At low oxygen concentrations (0.2%) benzene is primarily converted into  $CO_2$  via CO, whereas at high oxygen concentrations (20%) benzene is converted into  $CO_2$  via CO and HCOOH. After treatment, benzene fragments are deposited on the plane electrode and discharge chamber at low oxygen concentrations. It is found that an increase in the oxygen concentration inhibits the decomposition of benzene, which is also the case with a DBD discharge [74]. However, with a packed-bed reactor, a higher  $N_2/O_2$  ratio improves the decomposition of benzene [40] which indicates that the effect of the amount of oxygen in the background gas depends on the type of discharge.

Kim et al. [75] also investigated the influence of oxygen and found an optimum  $O_2$  concentration of 3–5% for benzene removal with a DBD discharge. Further increase of the oxygen concentration drastically decreases the decomposition efficiency. They suggest that higher benzene destruction at lower  $O_2$  partial pressure is due to the contribution of N radicals and excited  $N_2$  molecules. Comparison of the reaction rate constants indicates that the reaction with  $N_2(A^3\Sigma_u^+)$  is more plausible and is even faster than the reaction with O radicals ( $k = 1.6 \times 10^{-14} \text{ cm}^3 \text{ molecule}^{-1} \text{ s}^{-1}$ ). However, as  $O_2$  partial pressure increases, quenching of  $N_2(A^3\Sigma_u^+)$  becomes significant [76] and the rate of reaction slows down. In addition, more O atoms are produced due to direct electron-impact dissociation and collision dissociation by  $N_2(A^3\Sigma_u^+)$ , but at the same time O atoms are also consumed in the formation of  $O_3$ . Because the gas-phase reaction between ozone and benzene is very slow ( $k = 1.72 \times 10^{-22} \text{ cm}^3 \text{ molecule}^{-1} \text{ s}^{-1}$ ), it does not contribute to the decomposition of benzene.



$$k = 1.6 \times 10^{-10} \text{ cm}^3 \text{ molecule}^{-1} \text{ s}^{-1} \quad (37)$$





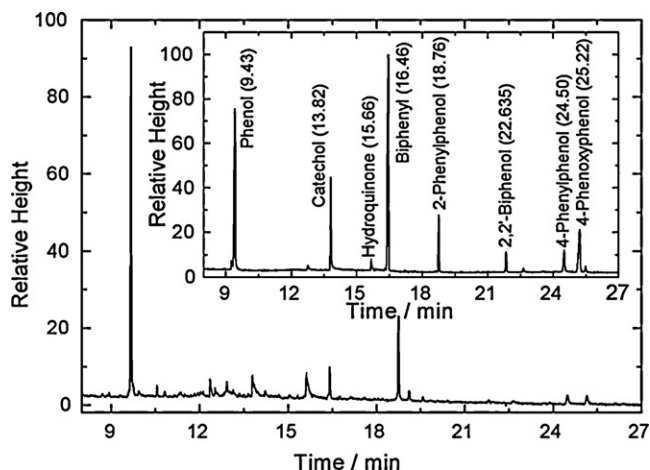


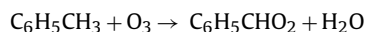
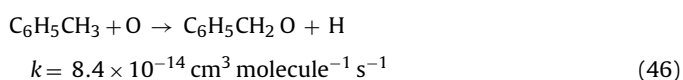
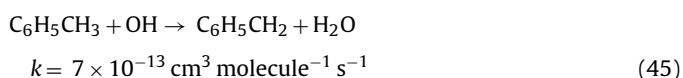
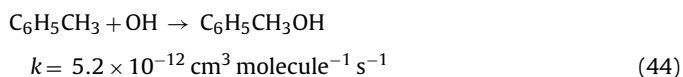
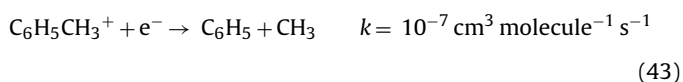
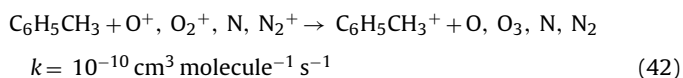
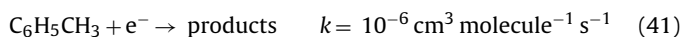
Fig. 4. Gas chromatogram of surface washed ethanolic solution from 10 min DBD discharge. Inset: Gas chromatogram of ethanolic solution of various standards employed.

Reprinted from Ref. [77], with permission from Elsevier.

In a recent study by Dey et al. [77] the formation of byproducts of benzene oxidation in a Ar/O<sub>2</sub> flow with a DBD reactor is carefully analyzed with GC–FID (flame ionization detector) and GC–MS. A plausible sequential reaction mechanism is given to rationalize the observation of the various byproducts. In the gas phase, only phenol and biphenyl are detected at a maximum conversion of 3%. GC analysis of an ethanolic solution of the polymeric deposit on the dielectric surface reveals the presence of substituted phenols besides phenol and biphenyl (Fig. 4). It is suggested that the intermediate phenyl radical plays the role of the primary precursor.

**2.1.3.3. Toluene.** Table 4 tends to give an overview of published work on toluene removal with the aid of NTP. Toluene can be regarded as the most studied VOC for abatement on laboratory scale. Therefore only a selection of papers will be discussed here. Other references can be found in Table 4.

Kohno et al. [78] have applied a DC capillary tube discharge reactor and investigated the effect of gas flow rate, initial toluene concentration and reactor operating conditions. According to the authors, the following destruction process can be expected in a NTP environment:



$$k = 1.5 \times 10^{-22} \text{ cm}^3 \text{ molecule}^{-1} \text{ s}^{-1} \quad (47)$$

FT-IR spectroscopy detects CO<sub>2</sub>, CO, NO<sub>2</sub> and H<sub>2</sub>O as gaseous byproducts and a significant amount of brown particles are deposited at the exit of the reactor. It is suggested that CO<sub>2</sub> and CO mainly form carbon and nitrogen hydride bonded aerosol particles and tars.

CO<sub>2</sub> and H<sub>2</sub>O are observed as main reaction products by Mista and Kacprzyk [79]. They also detect a thin polymeric film (brown residues) covering the discharge electrode and dielectric layer. Operation at higher energy densities can successively be applied to oxidize the condensed polymeric species to CO<sub>2</sub>. Machala et al. [80] suggest that formation of aerosols including peroxy-acetyl-nitrates species (PANs) may be possible during toluene removal through a mechanism that is similar to formation of photochemical smog in the atmosphere. In pure nitrogen [81], GC–MS analysis showed that N<sub>2</sub> plays a major role in the polymerisation process through the formation of C–N=C and C–(NH)–bonds. A proposal of the polymerisation process is given to explain the formation of micrometric sized particles in the plasma reactor.

In Ref. [82] a wire plate DBD has been used to examine the humidity effect on toluene decomposition. A maximum removal efficiency of 73% was achieved in a gas stream containing 0.2% H<sub>2</sub>O in N<sub>2</sub> with 5% O<sub>2</sub>. This controlled humidity is governed by two opposite effects: as humidity increases, more H<sub>2</sub>O molecules collide with high-energy electrons and form OH radicals, resulting in a higher removal efficiency. On the other hand, the electronegative characteristic of H<sub>2</sub>O limits the electron density in the plasma and quenches activated chemical species, as concluded by Van Durme et al. [83]. Kim et al. [75] have confirmed that 5% O<sub>2</sub> is the optimum oxygen partial pressure in a dry nitrogen stream, as is the case for benzene.

Recently, Schiorlin et al. [84] have tested three different corona discharges (positive DC, negative DC, positive pulsed) for toluene removal and have observed that process efficiency increases in the order positive DC < negative DC < positive pulsed. By investigating the effect of humidity on the removal efficiency, it is concluded that for both negative DC and positive pulsed corona, OH radicals are involved in the initial stage of toluene oxidation. When the RH was greater than 60%, removal efficiency slightly drops due to saturation and inhibition of the OH radical forming reactions, i.e. dissociation of H<sub>2</sub>O molecules induced by interaction with electrons or by reaction with O(<sup>1</sup>D).

A positive DC corona discharge has been applied by Van Durme et al. [83] in order to abate toluene from indoor air and to unravel the degradation pathway. The removal of toluene is achieved with a characteristic energy density of 50 J/L. Fig. 5 shows that partially oxidized intermediates are formed under the applied conditions. By determining the effect of humidity, the authors find out that OH radicals play a major role in the oxidation kinetics due to initiation by H-abstraction or OH-addition. The byproducts detected by GC–MS consist of benzaldehyde, benzylalcohol, formic acid, nitrophenols and furans.

## 2.2. Combined with catalyst

### 2.2.1. What is plasma-catalysis?

Many studies have shown that NTP is attractive for the removal of NO<sub>x</sub>, SO<sub>x</sub>, odours and VOCs. There is, however, a consensus among researchers that application of NTP for VOC abatement suffers from 3 main weaknesses, i.e. incomplete oxidation with emission of harmful compounds (CO, NO<sub>x</sub>, other VOCs), a poor energy efficiency and a low mineralization degree.

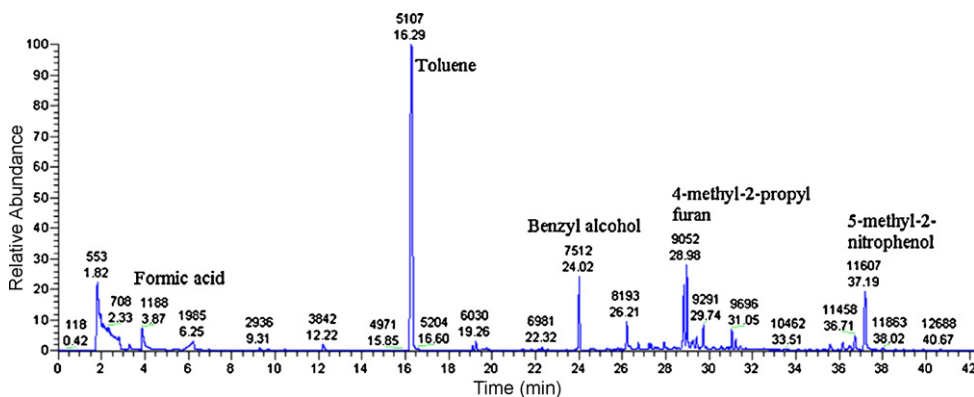


Fig. 5. Chromatogram of GC-MS analysis for the identification of toluene degradation products.

Reprinted from Ref. [83], with permission from Elsevier.

The combination of NTP with heterogeneous catalysts can be divided in two categories depending on the location of the catalyst: in-plasma catalysis (IPC) and post-plasma catalysis (PPC). The latter is a two-stage process where the catalyst is located downstream of the plasma reactor while the former is a single stage process with the catalyst being exposed to the active plasma. In literature, several different terms and corresponding abbreviations have already been proposed to represent IPC and PPC. For in-plasma catalysis, one can find among others: plasma-driven catalysis (PDC) [13], in-plasma catalysis reactor (IPCR) [85], single-stage plasma-catalysis (SPC) [86], plasma and catalyst integrated technologies (PACT) [87] or combined plasma catalysis (CPC) [88,89]. For PPC, the following terms have been proposed: plasma-enhanced catalysis (PEC) [13], post-plasma catalysis reactor (PPCR) [85], two-stage plasma catalysis (TPC) [86].

In plasma-catalysis, synergetic effects are related to the activation of the catalyst by the plasma. Activation mechanisms include ozone, UV, local heating, changes in work function, activation of lattice oxygen, adsorption/desorption, creation of electron-hole pairs and direct interaction of gas-phase radicals with adsorbed pollutants [75].

The plasma-catalyst interactions described in the following paragraphs contribute to one or more of these catalyst activation mechanisms. The presented experimental findings, applying to specific working conditions, may appear as scattered pieces of information. Indeed further research is needed to connect the loose ends and unravel the detailed mechanisms. However, it is meaningful to try and extract some general pathways at this stage.

**2.2.1.1. Influence of the catalyst on the plasma processes. Discharge mode:** The physical properties of a discharge will be affected if a catalyst is introduced into the discharge zone. When for example a dielectric surface is introduced in the gap of a streamer-type discharge, the discharge mode at least partially changes from bulk streamers to more intense streamers running along the surface (surface flashover) [90]. Similar field effects can lead to higher average electron energies when the discharge zone is filled with ferroelectric pellets, leading to a more oxidative discharge [91]. Parameters that influence the effect of the packed bed on the discharge are the dielectric constant of the pellet material and the size and shape of the pellets. The dielectric constant affects the electric field in the void between the pellets and thereby the mean electron energy. With increasing pellet size the number of microdischarges decreases, but the amount of charge that is transferred per microdischarge increases [92].

**Reactive species production:** Obviously, introducing a heterogeneous catalyst changes the physical characteristics of the discharge, so the chemical activity will be affected as well. Roland et al. [18]

studied the oxidation of various organic substances immobilized on porous and non-porous alumina and silica catalysts and concluded that short-living active species are formed in the pore volume of porous materials when exposed to NTP. On the other hand, introducing a catalyst can reduce the concentration of ionic species [93]. However, this effect did not impair the catalyst's role in reducing the emissions of ozone and carbon monoxide for this particular application (indoor air control).

**2.2.1.2. Influence of the plasma on the catalytic processes. Catalyst properties:** Non-thermal plasmas are used for catalyst preparation [94–99]. Plasma treatment of the catalyst enhances the dispersion of active catalytic components [100,101] and influences the stability and catalytic activity of the exposed catalyst material [102]. The oxidation state of the catalyst can also be altered by NTP. For instance, when a  $Mn_2O_3$  catalyst is exposed for a long time to a DBD plasma, X-ray diffraction spectra reveal the presence of  $Mn_3O_4$ , a lower-valent manganese oxide with a larger oxidation capability. Due to plasma-catalyst interactions, less parent Ti–O bonds are found on  $TiO_2$  surfaces after several hours of discharge operation [103]. Even new types of active sites with unusual properties may be formed [104], such as stable  $Al-O-O^*$  with a lifetime exceeding more than two weeks, as observed in the pores of  $Al_2O_3$  in IPC experiments [104]. Plasma exposure can result in an increase or decrease of the specific surface area or in a change of catalyst structure [100,102,105].

**Adsorption:** Adsorption processes play an important role in plasma-catalytic reaction mechanisms. If the catalyst has a significant adsorption capacity for pollutant molecules, it prolongs the pollutant retention time in the reactor. In the case of IPC, the pollutant concentration in the discharge zone is increased. The resulting higher collision probability between pollutant molecules and active species enhances the removal efficiency. Adsorption of VOC and active species increases with the porosity of the catalyst [106]. Under conditions where plasma-generated ozone is not effective in itself to destroy pollutants, high decomposition rates are obtained due to the adsorption of ozone on the catalyst surface and the subsequent dissociation into atomic oxygen species [107]. Humidity is a critical parameter in plasma-catalytic processes. The adsorption of water on the catalyst surface results in a decrease of the reaction probability of the VOC with the surface and therefore reduces the catalyst activity [82].

**Thermal activation:** Although gas heating will result in higher catalyst surface temperatures [108], the heating effect is in general too small to account for thermal activation of the catalyst. However, hot spots can be formed in packed-bed reactors as a result of localized heating by intense microdischarges that run between

sharp edges and corners of adjacent pellets. Increased catalyst temperatures can promote catalytic VOC removal [109].

**Plasma-mediated activation of photocatalysts:** In photocatalysis, VOCs are adsorbed on the surface of a porous semiconductor material that is exposed to UV radiation. The UV photons generate electron–hole pairs, inducing the subsequent oxidation of the adsorbed VOC by valence band holes. In a final step the oxidation products are desorbed. Among other photocatalysts (e.g. ZnO, ZnS, CdS, Fe<sub>2</sub>O<sub>3</sub>, WO<sub>3</sub>), TiO<sub>2</sub> is one of the most efficient for the decomposition of a wide range of VOCs. Moreover, the combination of TiO<sub>2</sub> with NTP results in higher oxidation efficiencies and better selectivity to CO<sub>2</sub>. For the anatase phase of TiO<sub>2</sub>, having a bandgap of 3.2 eV, it takes a photon with a wavelength shorter than 388 nm to create an electron–hole pair. Although there are excited nitrogen states that emit light in this wavelength range, there is experimental evidence that photocatalysis induced by UV light from the plasma cannot explain the observed synergy in several hybrid plasma/TiO<sub>2</sub> systems reported in literature. For instance, Sano et al. [110] has detected no enhancement in acetylene conversion when the reactor walls are coated with TiO<sub>2</sub>. Emission spectra of the surface discharge plasma with and without catalyst coating reveal that UV light from the plasma is absorbed by TiO<sub>2</sub>, but the intensity is too weak for photoactivation. This observation has been confirmed by Huang et al. [111], who employed a wire-cylinder DBD reactor with a photocatalyst sheet stuck along the inner wall of the tube. Kim et al. have tested a DBD reactor packed with Ag/TiO<sub>2</sub> for benzene removal [112]. When O<sub>2</sub>–benzene mixtures are diluted with argon, significantly higher decomposition efficiencies are observed compared to N<sub>2</sub> dilution. This result suggests that the role of UV light for photoactivation is negligible because light emission from excited argon ranges in the visible range (400–850 nm). However, other groups report that UV light emitted from the plasma can act as a source for activation of TiO<sub>2</sub> [70,113,114]. Subrahmanyam et al. [115] suggest that the increased activity with sintered metal fibres modified with TiO<sub>2</sub> might be related to activation as well as to photocatalytic action in the presence of UV light emitted by the plasma discharge. In some cases, TiO<sub>2</sub> shows plasma-induced catalytic activity under conditions where there is no or very little UV emitted by the plasma [112,116]. Direct plasma activation has been observed when TiO<sub>2</sub> is exposed to an atmospheric pressure argon discharge at room temperature [117]. The question then arises how the plasma-exposed TiO<sub>2</sub> is activated, if not by UV photons. Different mechanisms to bridge the TiO<sub>2</sub> band-gap by plasma-driven processes can be envisaged, but to date there is insufficient information to elaborate on the relative importance of electrons, ions, metastables, charging effects, surface recombination, etc.

### 2.2.2. Different types of catalysts

As in classical heterogeneous catalysis, the catalyst material can be introduced in the hybrid system in different ways for both IPC (Fig. 6) and PPC: in the form of pellets (a so-called packed-bed configuration) [91,118–121], foam [82,100,122,123,102] or honeycomb monolith [93,124–127], as a layer of catalyst material [128] or as a coating on the reactor wall [110,129] or electrodes [115,130–135].

Many catalysts have been tested for VOC abatement with IPC and PPC. Historically, the first materials tested were porous adsorbents placed inside the discharge region as in references [41,136]. The idea is that, by introducing these materials, the retention time of VOC molecules would increase along with the probability of surface reactions with active chemical plasma species (electrons, radicals, ions, photons). Adsorbents that were used to achieve a more complete oxidation are  $\gamma$ -Al<sub>2</sub>O<sub>3</sub> [17,18,136,137] and zeolites or molecular sieves [17,138–142]. Furthermore, these materials are coated or impregnated with (noble) metals such as silver, palladium, platinum, rhodium, nickel, molybde-

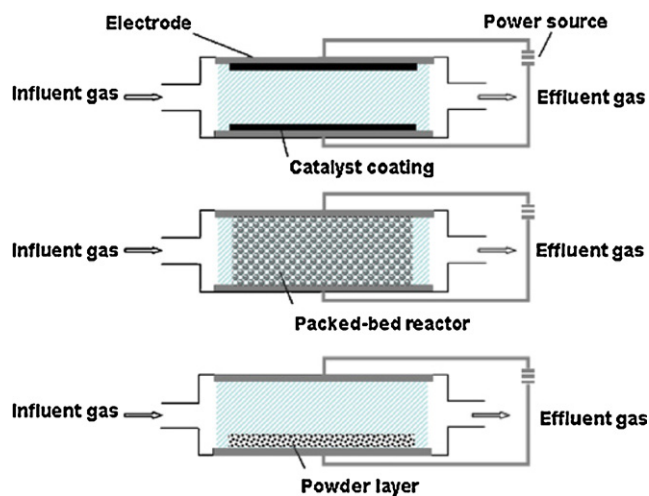


Fig. 6. Most common catalyst insertion methods for IPC configuration. Reprinted from Ref. [228], with permission from Elsevier.

num, copper, cobalt or manganese to provide catalytic activity [75,105,107,109,142–151]. Adsorbents also function as support for metal oxides [20,149,152–158].

Extensive attention has been given during recent years to the use of photocatalysts, in particular to TiO<sub>2</sub>. In most studies, TiO<sub>2</sub> is inserted in the discharge region in order to achieve activation through different mechanisms. This catalyst has also been coated with (noble) metals [67,75,107,112,116,159,160] and metal oxides [138,161–163]. Additionally, it has been used as a coating on activated carbon filter [111] or fibre [164], on glass fibres [165,166] or beads [70,113,167], nickel foam [168], silica gel pellets [129] and on UV lamp [169].

### 2.2.3. VOC abatement

Tables 6–9 give a summary of literature on VOC removal with plasma–catalysis. For each paper catalyst information and operating conditions are presented along with the maximum removal efficiency and energy density. In this section, particular attention is again paid to the most studied target compounds, i.e. trichloroethylene, benzene and toluene. Table 9 presents a list of other relevant, but less frequently studied VOCs that have been examined in plasma–catalytic studies. For more details about operating conditions and results, the reader can consult the corresponding references.

**2.2.3.1. Trichloroethylene.** Table 6 presents published papers regarding TCE abatement. Oda et al. [162] have investigated the effect of TCE initial concentration, pellet size and sintering temperature for TiO<sub>2</sub> catalysts on the TCE decomposition performance. When the barrier type reactor was filled with TiO<sub>2</sub> sintered at 673 K, the breakdown voltage to generate NTP greatly reduces in comparison to the empty reactor and the reactor filled with TiO<sub>2</sub> sintered at 1373 K. They suggest that the nonuniform geometrical distribution of the disk-like dielectric pellets sintered at 673 K disturbed the electric field and generated an electric field concentration at the contacting area of the pellets. This results in the formation of contacting point discharges or surface discharges on the pellet surfaces, lowering the breakdown voltage and improving the decomposition energy efficiency. Moreover, they indicate that too fine TiO<sub>2</sub> particles disturb the gas flow and cause insufficient filling of the discharge area with plasma.

In another study by Oda et al. [170], MnO<sub>2</sub> is used as a post-plasma catalyst in a direct (contaminated air is directly processed by the plasma) and an indirect process (plasma-processed clean air is mixed with the contaminated air). Manganese oxide is very effi-

**Table 6**  
Overview of published papers on TCE removal with plasma–catalysis.

Plasma type	Catalyst	Position	$T_{\text{cat}}$ (K)	Carrier gas	Flow rate (mL/min)	Concentration range (ppm)	Maximum removal efficiency (%)	Energy density (J/L)	References
DBD	MnO <sub>2</sub>	PPC	293	Air	500	250	95–99	240	[65]
DBD	TiO <sub>2</sub> /SMF	IPC	–	Air	700	250	>99	–	[131]
	CoO <sub>x</sub> (3 wt%)/SMF								
	MnO <sub>x</sub> (3 wt%)/SMF								
	TiO <sub>2</sub> /MnO <sub>x</sub> /SMF								
DBD	MnO <sub>x</sub> (3 wt%)/SMF	IPC	293	Air	500	150–200	95–99	550	[133]
DBD	MnO	IPC	293	Dry air	1000	250	>99	120	[144]
DBD	TiO <sub>2</sub>	IPC	293	Dry air	400	100	>99	180	[161]
	V <sub>2</sub> O <sub>5</sub> (0.7 wt%)/TiO <sub>2</sub>						95–99	140	
	V <sub>2</sub> O <sub>5</sub> (4.6 wt%)/TiO <sub>2</sub>						90–95	140	
	WO <sub>3</sub> (4.2 wt%)/TiO <sub>2</sub>						>99	180	
DBD	TiO <sub>2</sub> sintered at 1373 K	IPC	293	Dry air	400	1000			[162]
	0.5–1 mm						>99	200	
	1–2 mm						>99	120	
	2–3 mm						>99	120	
	TiO <sub>2</sub> sintered at 673 K						>99	120	
DBD	MnO <sub>2</sub>	IPC	293	Dry air	400	1000	>99	120	[170]
DBD	Au/SBA-15	PPC	–	Dry air	510	430	>99	670	[172]
DC positive corona	TiO <sub>2</sub>	IPC	–	Dry air	1500	100	85	600	[118]
DC negative glow	Pd(0.05 wt%)/Al <sub>2</sub> O <sub>3</sub>	PPC	373	Humid air	2000	600–700	80	300	[147]
Surface discharge	V <sub>2</sub> O <sub>5</sub> /TiO <sub>2</sub>	IPC	293	Dry air	400	1000	>95	50	[143]
	Cu–ZSM-5						>95	50	

cient in enhancing the decomposition efficiency for both processes. The catalysts effectiveness to dissociate ozone generates oxygen radicals which are excellent oxidizers for TCE removal.

Han et al. [171] have further examined the effect of the manganese dioxide post-plasma catalyst for the direct and indirect process. For the direct process oxygen species, generated from collisions between excited species (or electrons) with O<sub>2</sub>, mainly oxidize TCE into DCAC. The increased decomposition efficiency for the direct process is ascribed to the oxidation of the remaining TCE into trichloroacetaldehyde (CCl<sub>3</sub>–CHO, TCAA) by oxygen species produced during ozone decomposition at the surface of MnO<sub>2</sub>. The CO<sub>x</sub> yield increases from 15% to 35% at an energy density of 120 J/L when MnO<sub>2</sub> is present. When the energy density is raised to 400 J/L, a CO<sub>x</sub> yield of 98% is established. For the indirect process, similar

conclusions are made although the CO<sub>x</sub> yield is not as good as for the direct process.

Magureanu et al. [133] have tested a plasma–catalytic DBD reactor with an inner electrode made of sintered metal fibres (SMF) coated by transition metal oxides. Fig. 7 shows the CO and CO<sub>2</sub> selectivity over the range of energy densities used. The selectivity to CO<sub>2</sub> reaches 25% with the SMF and showed a significant improvement with MnO<sub>x</sub>/SMF, up to 60%. The use of MnO<sub>x</sub>/SMF does, however, not substantially lower the selectivity to CO. Thus, as compared to the reactor with SMF electrode, TCE conversion and CO<sub>2</sub> selectivity were significantly enhanced using MnO<sub>x</sub>/SMF. The ability of MnO<sub>2</sub> to decompose ozone *in situ*, produces strong oxidizing atomic oxygen species on the catalyst surface. These species may lead to an enhanced oxidation of TCE resulting in a high CO<sub>2</sub> selectivity [115,131,133]. After reaction, XPS (X-ray photoelectron spectroscopy) analysis of the catalyst has revealed that both manganese and iron have preserved their initial oxidation state. The used catalyst, however, shows an enrichment of iron on the catalyst surface suggesting a redispersion of manganese on the surface during reaction. Finally, XPS also reveals some chlorine deposition on the catalyst surface after reaction.

In another study conducted by Magureanu et al. [172], gold nano-particles embedded in SBA-15 have been tested for PPC. The catalyst with the least amount of Au (0.5 wt%) seems to enhance the CO<sub>x</sub> selectivity the most and has the best catalytic performance. As for MnO<sub>2</sub>, the Au/SBA-15 can dissociate ozone, produced in the plasma, to oxygen radicals that decompose TCE. They suggest that in the presence of ozone generated in the plasma, isolated gold cations are the active sites that elucidate the catalytic behaviour.

To achieve a more complete oxidation of TCE at a reduced energy cost, Morent et al. [118] have used a hybrid plasma–catalyst system with cylindrical TiO<sub>2</sub> pellets for IPC. They suggest that the increased removal fraction for the plasma–catalytic system can be explained through adsorption on and/or photoactivation of TiO<sub>2</sub>. Adsorption of TCE molecules on the surface of TiO<sub>2</sub> increases the residence time of TCE in the discharge.

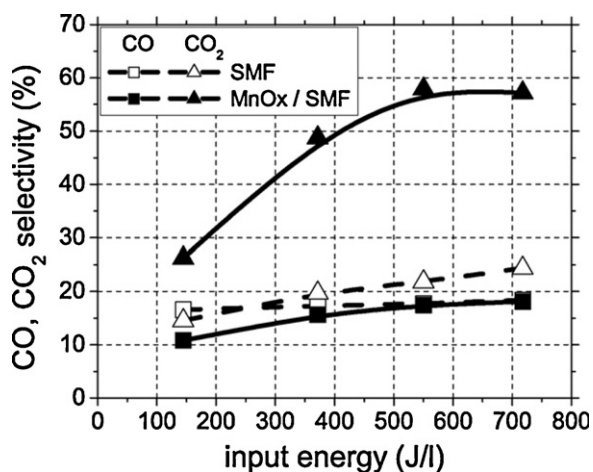


**Fig. 7.** Selectivity to CO and CO<sub>2</sub> as a function of input energy for inner electrodes made of SMF and MnO<sub>x</sub>/SMF.

Reprinted from Ref. [133], with permission from Elsevier.



**Table 7**  
Overview of published papers on benzene removal with plasma–catalysis.

Plasma type	Catalyst	Position	$T_{cat}$ (K)	Carrier gas	Flow rate (mL/min)	Concentration range (ppm)	Maximum removal efficiency (%)	Energy density (J/L)	References
DBD	TiO <sub>2</sub>	IPC	–	Dry air	100	100	60	900	[93]
	MnO <sub>2</sub>				500	105	54	360	
	TiO <sub>2</sub> –silica				500	105	50	320	
DBD	TiO <sub>2</sub>	IPC	293	Dry air	250	300–380	12	170	[108]
	MnO <sub>2</sub>						16	170	
DBD	TiO <sub>2</sub> Pt(1 wt%)/TiO <sub>2</sub> V <sub>2</sub> O <sub>5</sub> (1 wt%)/TiO <sub>2</sub>	IPC	–	Dry air	400	200	90 >99 >99	3150	[163]
DBD	Ag(2 wt%)/TiO <sub>2</sub>	IPC	373	Dry air	4000	110	>99	125	[176]
DBD	Kr/I <sub>2</sub> (Kr <sup>+</sup> excimer UV radiation)	IPC	293	Dry air	13 × 10 <sup>3</sup> –130 × 10 <sup>3</sup>	30–940	66.5	–	[230]
DBD	TiO <sub>2</sub>	IPC	293	Dry air	–	188	98	–	[262]
DBD glow discharge	TiO <sub>2</sub> /Al <sub>2</sub> O <sub>3</sub>	IPC	–	Dry air	200	100	50	140	[70]
Pulsed corona	silica gel	IPC	–	Dry air	100	300	85	–	[90]
Multistage corona <sup>a</sup>	TiO <sub>2</sub>	IPC	293	Dry air	60	1500	92.7	–	[222]
	Sol–gel TiO <sub>2</sub>						91.7		
	Pt/Sol–gel TiO <sub>2</sub>						>99		
Surface discharge	Ag(1 wt%)/TiO <sub>2</sub>	IPC	373	Dry air Humid air	200–3000	200–210	89	383	[67]
							86	391	
Surface discharge	Ag(4 wt%)/TiO <sub>2</sub>	IPC	373	Dry air	4000–10 <sup>4</sup>	200	>99	89–194	[75]
	Ni(2 wt%)/TiO <sub>2</sub>						>99		
	Ag(0.5/5 wt%)/Al <sub>2</sub> O <sub>3</sub>						>99		
	Pt(0.5 wt%)/Al <sub>2</sub> O <sub>3</sub>						>99		
	Pd(0.5 wt%)/Al <sub>2</sub> O <sub>3</sub>						>99		
	Ferrierite						>99		
	Ag(2 wt%)/H–Y						>99		
Packed-bed DBD	TiO <sub>2</sub>	IPC	373	Dry air	2000	203–210	82	388	[174]
	Pt(1 wt%)/TiO <sub>2</sub>						80	391	
	V <sub>2</sub> O <sub>5</sub> (1 wt%)/TiO <sub>2</sub>						90	383	
BaTiO <sub>3</sub> packed-bed	TiO <sub>2</sub>	IPC	292	Dry air	1000	500	66	60	[180]
	Ag(0.5 wt%)/TiO <sub>2</sub>						60		
	Al <sub>2</sub> O <sub>3</sub>						52		
	Ag(0.5 wt%)/Al <sub>2</sub> O <sub>3</sub>						49		
	TiO <sub>2</sub>						34		
	Ag(0.5 wt%)/TiO <sub>2</sub>						46		
Al <sub>2</sub> O <sub>3</sub>	28								
Ag(0.5 wt%)/Al <sub>2</sub> O <sub>3</sub>	39								

<sup>a</sup> Four stages in serie.

To confirm the presence of excited species of nitrogen, Subrahmanyam et al. give an UV–vis emission spectrum of the DBD plasma discharge in the wavelength range 250–500 nm. It is proven that emission of excited nitrogen molecules (N<sub>2</sub><sup>\*</sup>) is in the range of the band gap of the TiO<sub>2</sub>/SMF catalyst [115]. They suggest that the increased activity of TiO<sub>2</sub>/SMF might be due to photocatalytic action in the presence of UV light as well as activation of TiO<sub>2</sub> by the plasma discharge.

Vandenbroucke et al. [147] have investigated the use of a DC glow discharge combined with Pd/γ-Al<sub>2</sub>O<sub>3</sub> located in an oven downstream. When the catalyst temperature was set at 373 K, the combined system showed synergistic effects on the removal of TCE. By comparing the experimental removal efficiency of the hybrid system with the removal calculated by multiplying the individual effects (plasma and catalyst alone), 12–22% additional TCE was decomposed. A more elaborated review on plasma–catalytic abatement of TCE can be found in [173].

**2.2.3.2. Benzene.** Ogata et al. [136] have performed much research on the removal of benzene with plasma–catalysis. In a first study, they test an adsorbent hybrid reactor packed with a mixture of BaTiO<sub>3</sub> and Al<sub>2</sub>O<sub>3</sub> pellets and compare the results with a BaTiO<sub>3</sub>

packed reactor and a two-stage reactor (BaTiO<sub>3</sub> packed reactor with Al<sub>2</sub>O<sub>3</sub> downstream). The hybrid reactor shows the best performance, owing to its better energy efficiency, CO<sub>2</sub>-selectivity and suppressed N<sub>2</sub>O formation. The combined effect of benzene concentration on Al<sub>2</sub>O<sub>3</sub> followed by surface decomposition and gas-phase reaction is thought to be responsible for the enhanced decomposition. Cyclic operation of adsorption and plasma discharge is suggested to further improve the energy efficiency. In Ref. [137] they continue examining a catalyst hybrid reactor with metal supported Al<sub>2</sub>O<sub>3</sub> and have found that Ag-, Co-, Cu and Ni-supported Al<sub>2</sub>O<sub>3</sub> shows a slightly better CO/CO<sub>2</sub> ratio and a lower N<sub>2</sub>O formation than the adsorbent hybrid reactor. Next, a zeolite hybrid plasma reactor (mixture of zeolite and BaTiO<sub>3</sub>) has been applied for dilute benzene decomposition [139]. The higher adsorption capacity of zeolite structures compared to alumina allows a higher decomposition efficiency and CO/CO<sub>2</sub> ratio if the micropore surface area is large enough for accommodation of benzene molecules. The authors have also found that benzene adsorbed outside of a zeolite crystalline pore decomposed more easily than that inside a zeolite pore. In Ref. [145] they expand the study and examine the effect of BaTiO<sub>3</sub> pellet size and mixing ratio of BaTiO<sub>3</sub> and adsorbent, catalyst or zeolite. Plasma energy is found to be almost independent of the pellet size. However, with pellets larger than 2 mm in diam-



**Table 8**  
Overview of published papers on toluene removal with plasma–catalysis.

Plasma type	Catalyst	Position	$T_{cat}$ (K)	Carrier gas	Flow rate (mL/min)	Concentration range (ppm)	Maximum removal efficiency (%)	Energy density (J/L)	References
DBD	Al <sub>2</sub> O <sub>3</sub>	IPC	293 373	Air (18% RH)	10 <sup>4</sup>	220	60–65 80	110	[17]
DBD	Fe <sub>2</sub> O <sub>3</sub> /MnO honeycomb	PPC	293	Dry air	2500	85	65	72	[127]
DBD	SMF CoO <sub>x</sub> (3 wt%)/SMF MnO <sub>x</sub> (3 wt%)/SMF	IPC	–	Air	500	250	60 70 65	160	[131]
DBD	SMF CoO <sub>x</sub> (3 wt%)/SMF MnO <sub>x</sub> (3 wt%)/SMF Cu	IPC	–	Air	500	500	90 92 95 90	298	[134]
DBD	MnPO <sub>4</sub> Mn–APO-5 Mn–SAPO-11	PPC	673	Air	50–150	560	70 65 70	900–2700	[142]
DBD	Ag/TiO <sub>2</sub>	IPC	373	Air	4000	101	95	125	[176]
DBD	Ti–MPS Mn(5 wt%)-Ti–MPS Mn(10 wt%)-Ti–MPS	PPC	–	Air	200	1000	45 58 75	300	[263]
Wire-cylinder DBD	TiO <sub>2</sub> /activated carbon filter	IPC	–	Air (0.5% H <sub>2</sub> O)	200	100	55	–	[111]
Wire-cylinder DBD	Al <sub>2</sub> O <sub>3</sub> TiO <sub>2</sub> /Al <sub>2</sub> O <sub>3</sub> MnO <sub>2</sub> (5 wt%)/Al <sub>2</sub> O <sub>3</sub> MnO <sub>2</sub> (10 wt%)/Al <sub>2</sub> O <sub>3</sub> MnO <sub>2</sub> (15 wt%)/Al <sub>2</sub> O <sub>3</sub>	IPC	–	Dry air	2000	186	75 86 84 96 96	700	[20]
Wire-cylinder DBD	TiO <sub>2</sub> /glass pellets	IPC	293	Dry air	600	1100	80	1000	[167]
Wire-plate DBD	TiO <sub>2</sub> /Al <sub>2</sub> O <sub>3</sub> /Ni foam	PPC	–	Dry air	200	50	95	900	[122]
Wire-plate DBD	MnO <sub>2</sub> /Al/Ni foam	IPC	–	5% O <sub>2</sub> /N <sub>2</sub>	100	50	>95	750	[100]
DBD (pulsed)	Mn-1 Mn-2 Mn-3	PPC	300	Air	300	200	90–95	1400	[264]
DBD packed with glass beads	N150 (MnO <sub>2</sub> –Fe <sub>2</sub> O <sub>3</sub> ) Al <sub>2</sub> O <sub>3</sub> MnO <sub>2</sub> (9 wt%)/Al <sub>2</sub> O <sub>3</sub> Activated carbon (AC) MnO <sub>2</sub> (3 wt%)/AC	PPC	–	Air	588	240	76 74 88 98.5 99.7	172	[202]
Multistage packed-bed DBD	MnO <sub>2</sub> MnO <sub>2</sub> –CuO	PPC	–	Air	10 <sup>4</sup>	70	>99 >99	340	[265]
BaTiO <sub>3</sub> packed-bed	Al <sub>2</sub> O <sub>3</sub> Ag <sub>2</sub> O(7 wt%)/Al <sub>2</sub> O <sub>3</sub> MnO <sub>2</sub> (7 wt%)/Al <sub>2</sub> O <sub>3</sub> Al <sub>2</sub> O <sub>3</sub> Ag <sub>2</sub> O(7 wt%)/Al <sub>2</sub> O <sub>3</sub> MnO <sub>2</sub> (7 wt%)/Al <sub>2</sub> O <sub>3</sub>	IPC  PPC	673 573 603 698 573 603	Dry air	1000	500	95 >99 >99 78 >99 >99	60	[153]
BaTiO <sub>3</sub> packed-bed	TiO <sub>2</sub> Al <sub>2</sub> O <sub>3</sub> Ag(0.5 wt%)/Al <sub>2</sub> O <sub>3</sub> TiO <sub>2</sub> Al <sub>2</sub> O <sub>3</sub> Ag(0.5 wt%)/TiO <sub>2</sub> Ag(0.5 wt%)/Al <sub>2</sub> O <sub>3</sub>	IPC  PPC	753  886	Dry air	1000	500	91 >99 >99 95 >99 95–99 99	60	[180]
Pulsed corona	Pt-honeycomb	PPC	513	Air	2 × 10 <sup>4</sup>	330	90–95	142	[126]
Pulsed corona	Reticulated vitreous carbon Pt/Rh coated electrodes	IPC	433	Dry air	1000	200	85	140–150	[130]
Pulsed corona	AlO <sub>2</sub> Silica gel	IPC	–	Air	100	300	>95	5.43.5	[90]
Pulsed corona	Al <sub>2</sub> O <sub>3</sub>	IPC	–	Air	400	1100	>99	1100	[181]
DC positive corona	TiO <sub>2</sub>	IPC PPC	–	Air	1000	80–100	75 70	160 330	[182]
DC positive corona	TiO <sub>2</sub> CuO–MnO <sub>2</sub> /TiO <sub>2</sub>	IPC PPC	293	Dry air	10 <sup>4</sup>	0.5	82 78	17 2.5	[186]
DC positive corona	Cu–Mn/TiO <sub>2</sub> (a) N140 N150 Pd(0.5 wt%)/Al <sub>2</sub> O <sub>3</sub> Cu–Mn/TiO <sub>2</sub> (b)	PPC	293	Air (50% RH)	10 <sup>4</sup>	0.5	40 47 34 47 62	14 16 16 10 20	[107]

Table 8 (Continued)

Plasma type	Catalyst	Position	$T_{\text{cat}}$ (K)	Carrier gas	Flow rate (mL/min)	Concentration range (ppm)	Maximum removal efficiency (%)	Energy density (J/L)	References
Wire-cylinder corona	TiO <sub>2</sub> (3 wt%)/glass beads TiO <sub>2</sub> (3 wt%)/Al <sub>2</sub> O <sub>3</sub>	IPC	–	10% O <sub>2</sub> /N <sub>2</sub>	4000	1000	70–75 80–85	–	[113]
Positive DC streamer	Cu–Mn/Al <sub>2</sub> O <sub>3</sub>	PPC	573	Air	$133 \times 10^3$	45	96	20	[146]
Surface discharge	Ni/cordierit honeycomb Mn–Cu/cordierit honeycomb V/cordierit honeycomb	PPC	–	Air	$666 \times 10^3$	30	40–45	–	[93]
Surface discharge	zeolites	IPC	–	Air (0.5% H <sub>2</sub> O)	500	200	–	–	[140]
Pulsed wire-cylinder DBD	Pt/Al <sub>2</sub> O <sub>3</sub>	IPC	468	Air	$2 \times 10^4$	300	92	–	[266]

eter sparking occurs earlier. For the catalyst hybrid reactor (with metal supported Al<sub>2</sub>O<sub>3</sub>), larger BaTiO<sub>3</sub> pellets in comparison to catalyst pellets, are beneficial because high-energy plasma is formed around the contact points of the BaTiO<sub>3</sub> pellets (Fig. 8). This shows the importance of the combination method to effectively induce catalytic properties.

Kim et al. have also tested various catalyst formulations and reactor types to enhance the decomposition of benzene with NTP. A BaTiO<sub>3</sub> packed-bed reactor has been modified by replacing the ferroelectric material with TiO<sub>2</sub>, Pt/TiO<sub>2</sub> or Ag/TiO<sub>2</sub> pellets [174]. The reactor is placed in an oven that controls the temperature at 373 K. Experiments reveal that the catalytic activity for benzene decomposition is in the order Ag/TiO<sub>2</sub> > TiO<sub>2</sub> > Pt/TiO<sub>2</sub>. The silver catalyst also improves the CO<sub>2</sub>-selectivity with 15% compared to the BaTiO<sub>3</sub> packed-bed reactor. Beside CO<sub>2</sub> and CO, no other byproducts are formed, which is confirmed by good carbon balances. Results indicate that the energy density is the governing factor for benzene decomposition rather than the amount of Ag/TiO<sub>2</sub> (grams of catalyst) in the reactor [175] or the gas residence time [176]. However, larger amounts of Ag/TiO<sub>2</sub> slightly reduce the formation of N<sub>2</sub>O. In this study, formic acid is found as minor byproduct at lower energy density. While a pulsed corona and surface discharge reactor form aerosols during benzene removal, negligible amounts are detected in the reactor packed with Ag/TiO<sub>2</sub> [175]. In a subsequent study [177], Ag-loading amount on TiO<sub>2</sub> (percentage of Ag on catalyst) confirms to have no effect on the benzene removal. This parameter,

however, plays an important role for the oxidative decomposition of intermediates on the TiO<sub>2</sub> surface, indicated by the carbon balance. Larger Ag-loading seems to benefit the carbon balance and CO<sub>2</sub>-selectivity. Further work has examined the activation mechanism of the Ag/TiO<sub>2</sub> catalyst in the hybrid reactor [112]. Thermal catalytic experiments and comparison of the effects of dilution gases (Ar, N<sub>2</sub>) on benzene removal respectively reveal that temperature is not an important parameter and contribution of plasma generated UV light to the photoactivation of the catalyst is negligible. The authors therefore suggest that *in situ* decomposition of ozone over Ag/TiO<sub>2</sub> and plasma-induced catalysis at higher energy density play a dominant role. The observed zero-order kinetics to benzene concentration supports the latter assumption. The catalyst shows good durability against catalyst deactivation for over 150 h of continuous operation tests [176].

Finally, Kim et al. [75] have tested a cycled system of adsorption and oxygen plasma as earlier proposed by Ogata et al. [136] and Song et al. [17]. Benzene oxidation is examined as function of oxygen partial pressure (0–80% O<sub>2</sub>) and different catalyst types (TiO<sub>2</sub>,  $\gamma$ -Al<sub>2</sub>O<sub>3</sub>, zeolites) inside the reactor. An increase of O<sub>2</sub> partial pressure improves both the decomposition and CO<sub>2</sub>-selectivity of benzene regardless of the catalyst used. Tests with the cycled system demonstrate that the regeneration mode must be done with pure oxygen to fully suppress harmful N<sub>x</sub>O<sub>y</sub> formation. The authors suggest a plausible reaction mechanism where removal of benzene mainly proceeds on the surface of the main catalysts (Fig. 9).

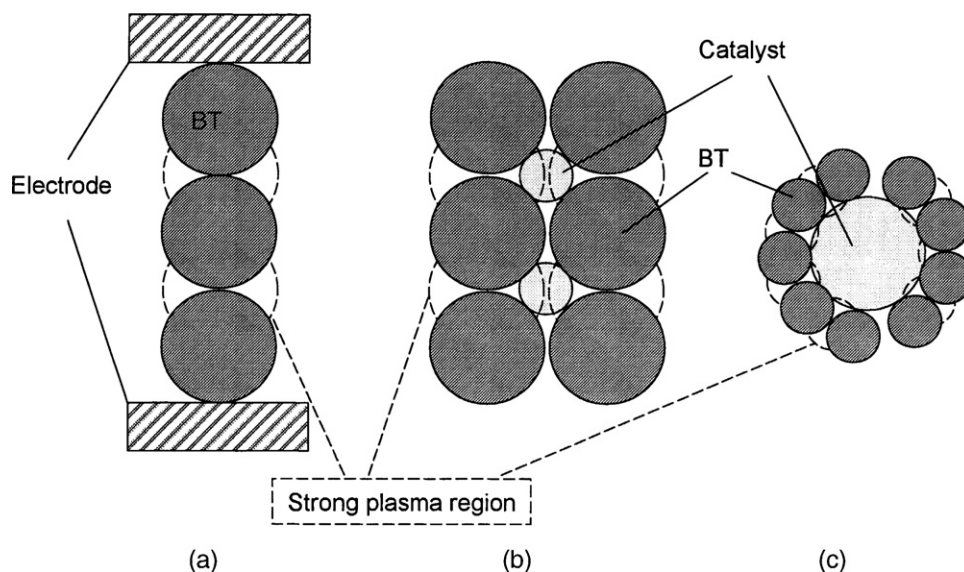


Fig. 8. Image of plasma discharge in a (a) BaTiO<sub>3</sub> packed-bed DBD and in hybrid reactors with mixtures of (b) BaTiO<sub>3</sub> > catalyst and (c) BaTiO<sub>3</sub> < catalyst. Reprinted from Ref. [145], with permission from Elsevier.

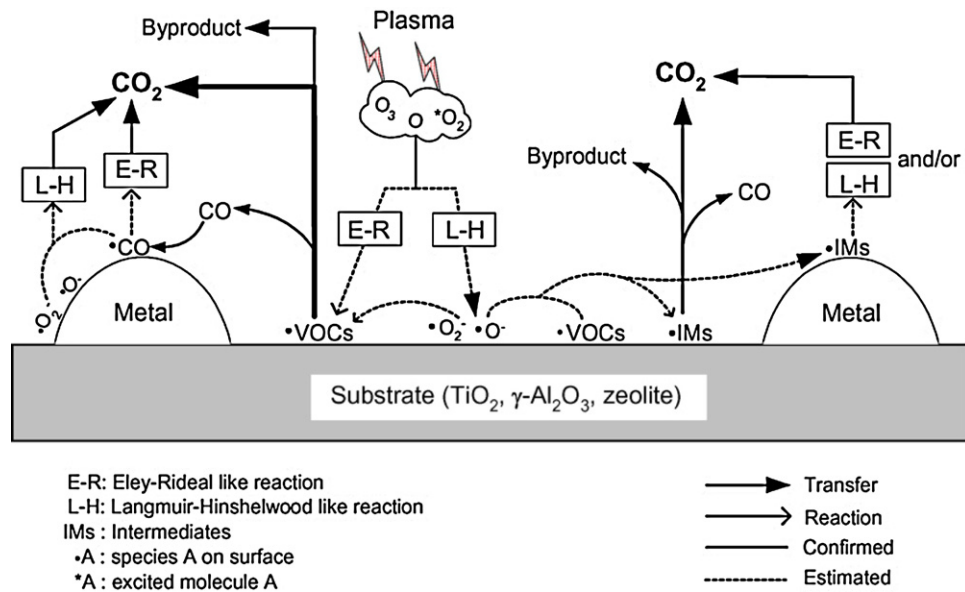


Fig. 9. Plausible mechanism for IPC for VOCs on various catalysts.

Reprinted from Ref. [75], with permission from Elsevier.

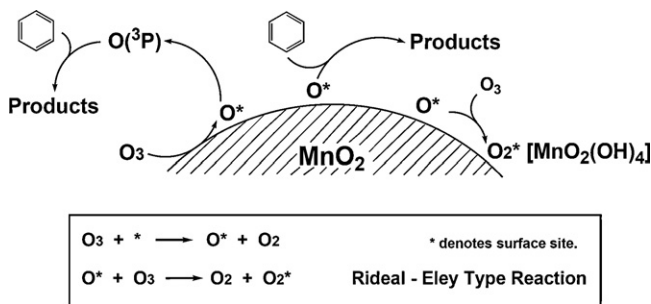


Fig. 10. Mechanism for  $MnO_2$ -catalyzed oxidation of benzene.

Reprinted from Ref. [129], with permission from Elsevier.

Recently, Fan et al. [178] have also investigated a cycled system with a storage and a discharge stage packed with a metal supported zeolite (Ag/HZSM-5). High oxidation rate of adsorbed benzene as well as low energy cost ( $3.7 \times 10^{-3}$  kWh/m<sup>3</sup>) are achieved at a moderate discharge power. Additionally, Ag/HZSM-5 exhibited good stability during cycled operation.

In a study by Futamura et al. [129], a DBD discharge is applied to investigate the synergistic effect of filling the plasma reactor with different catalysts ( $TiO_2$ ,  $MnO_2$  and  $TiO_2$ -silica gel). They suggest a mechanism for  $MnO_2$ -catalyzed oxidation of benzene (Fig. 10). Apparently, adsorption of ozone forms oxygen atoms on the  $MnO_2$

surface which partially desorb as  $O(^3P)$  in the gas phase, acting as possible oxidants for benzene decomposition.

Park et al. [163] have attached sheet type catalysts ( $TiO_2$ ,  $Pt/TiO_2$  and  $V_2O_5/TiO_2$ ) on the dielectric barrier of a DBD discharge. Benzene decomposition efficiency decreases in the order  $V_2O_5/TiO_2 > Pt/TiO_2 > TiO_2$ . Suppression of  $N_2O$  formation and improved mineralization degrees are obtained with all catalysts. Results indicate that high-energy electrons along with UV light generated from DBD plasma excite the  $TiO_2$  catalysts.

A hybrid plasma-photocatalyst system has also been tested by Lee et al. [70]. Comparison of OES (optical emission spectroscopy) spectra of the DBD glow discharge and an UV lamp confirms that the discharge emits UV light with an energy corresponding to 3–4 eV. The authors assume that photocatalysis could be possible using plasma as a photoactivation source, as proposed by Park et al. [163]. Titanium dioxide is coated on glass beads and on three types of  $\gamma-Al_2O_3$  with different surface area, pore volume and pore diameter. High porous alumina dramatically enhances the benzene conversion and mineralization degree.

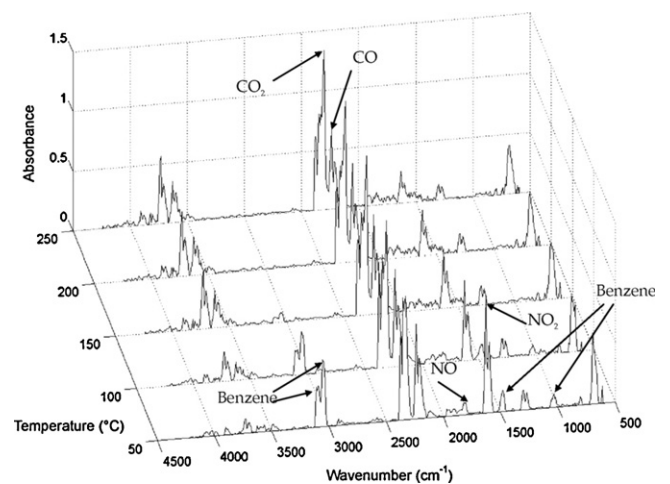


Fig. 11. FT-IR spectra showing the plasma-catalytic destruction of benzene with  $Ag/\gamma-Al_2O_3$ , as a function of temperature in a two-stage configuration.

Reprinted from Ref. [180], with permission from Elsevier.

Table 9

Published papers on removal of other VOCs with plasma-catalysis.

Target VOC	References
Acetaldehyde	[110,267,268]
Acetone	[91,160,167]
Acetylene	[106,165,166,241,269]
Dichloromethane	[105,144,270,271]
Formaldehyde	[220,272]
Methane	[90,148,273]
Methanol	[249]
Propane	[17,149,157]
Propene	[149]
Styrene	[151,176,274,275]
Tetrachloromethane	[150,198]
Xylene	[159,176,276–282]

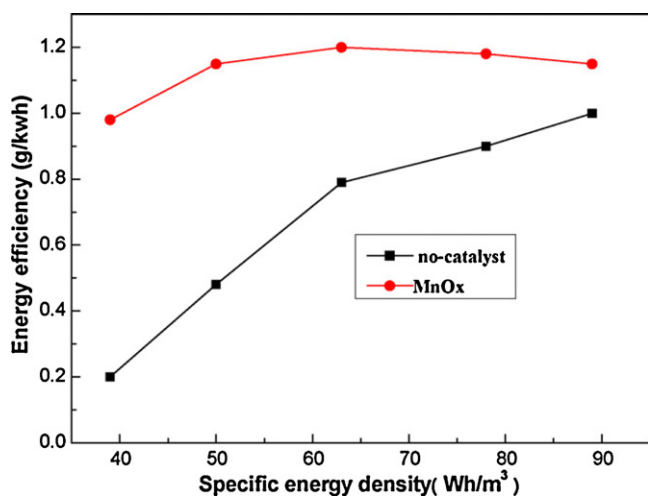


Fig. 12. Effect of energy density on energy yield of different catalysts (RH: 20%; initial toluene concentration: 105 ppm; gas flow rate: 450 mL/min).

Reprinted from Ref. [183], with permission from Elsevier.

In Ref. [179] the influence of humidity on benzene removal is investigated with a DBD packed with Raschig rings coated with nano TiO<sub>2</sub> films. Humidity negatively affects decomposition of benzene for three reasons: deactivation of high-energy electrons, inhibition of ozone formation and suppression of the catalyst activity of TiO<sub>2</sub> for benzene oxidation with ozone.

Harling et al. [180] have examined the effect of temperature (293–886 K) and catalyst position (IPC/PPC). Fig. 11 shows IR spectra of the plasma-catalytic destruction of benzene as a function of temperature with Ag/γ-Al<sub>2</sub>O<sub>3</sub> in a two-stage configuration. When compared to thermal catalysis, NO<sub>x</sub> formation is detected and increasing amounts are produced at elevated temperatures. Additionally, higher levels of destruction are observed at lower temperatures for plasma-catalysis.

**2.2.3.3. Toluene.** Table 8 gives an extensive overview of the papers that have been published on the plasma-catalytic abatement of toluene. A concise discussion is given on selected papers. Other references can be found in Table 8.

Song et al. [17] have applied a DBD packed with macro-porous γ-Al<sub>2</sub>O<sub>3</sub> and investigated the effect of adsorption and elevated temperature. Higher operating temperatures (373 K) cause a reduction in adsorption capability. However, toluene removal is more favorable under these conditions in comparison with the use of non-adsorbing glass beads. The use of γ-Al<sub>2</sub>O<sub>3</sub> beads proves to reduce some of the gas-phase byproducts, such as O<sub>3</sub> and HNO<sub>3</sub>, generated by the NTP process. Malik and Jiang [181] have also indicated that selecting the alumina packing with higher overall surface area can lower ozone generation without affecting the destruction efficiency of toluene.

In a study by Li et al. [182], a DC streamer corona discharge is employed in combination with TiO<sub>2</sub> pellets. Positioning the photocatalyst between the needle and mesh electrodes benefits the plasma discharge due to a higher streamer repetition rate. This configuration shows the best performance for decomposition (76%) and energy efficiency (7.2 g/kWh). This is attributed to the simultaneous decomposition of gas phase and adsorbed toluene and to possible TiO<sub>2</sub> activation by plasma inducing catalytic reactions. In absence of the TiO<sub>2</sub> layer, both the decomposition (44%) and efficiency (3.2 g/kWh) significantly drop. The authors claim that intermittent operation can improve the efficiency due to the regeneration of the catalyst surface through desorption during the discharge.

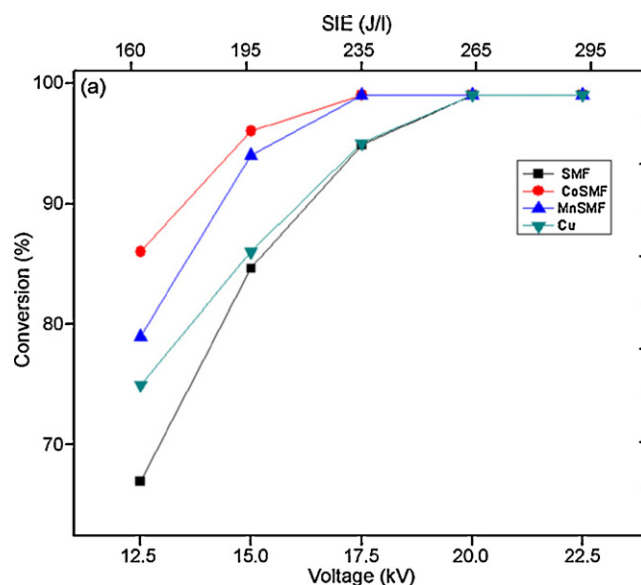


Fig. 13. Influence of SMF modification and energy density on the conversion of 100 ppm toluene.

Reprinted from Ref. [134], with permission from Elsevier.

Guo et al. [183] have applied a DBD to study the effect of MnO<sub>x</sub>/Al<sub>2</sub>O<sub>3</sub>/nickel foam for IPC. Earlier results have confirmed that MnO<sub>x</sub>/Al<sub>2</sub>O<sub>3</sub>/nickel foam is the most effective for toluene removal among different catalysts tested [102]. Fig. 12 shows that the MnO<sub>x</sub> catalyst greatly improves the energy yield as compared to the plasma-alone system. A sampling method has been developed to detect OH radicals in the gas phase and on the catalyst surface [184]. The catalyst can enhance the toluene removal efficiency due to efficient reactions of OH radicals with toluene on the surface or the active sites and other active species on the catalyst. With the plasma-catalytic system toluene removal decreases with increased humidity. It is suggested that water molecules cover the catalyst surface, resulting in a lower reaction probability [185]. Indeed, Van Durme et al. [186] have concluded that water molecules adsorb on the catalyst surface to form mono- or multi-layers that block active sites and create an extra diffusion layer for toluene to reach the catalyst surface. This hypothesis has also been confirmed by Huang et al. [122,123]. In a recent paper [187], Huang et al. have investigated the effect of water vapor on toluene removal efficiency, carbon balance, CO<sub>2</sub> selectivity and outlet ozone concentration. A wire-plate DBD filled with MnO<sub>x</sub>/Al<sub>2</sub>O<sub>3</sub>/nickel foam or TiO<sub>2</sub>/Al<sub>2</sub>O<sub>3</sub>/nickel foam is used to perform experiments. The results show that increased humidity lowers the formation of ozone through quenching of energetic electrons. Also, catalytic decomposition of ozone is depressed by the presence of water vapor due to competitive adsorption causing deactivation of the catalyst and suppression of catalytic ozonation. The carbon balance and CO<sub>2</sub> selectivity reach maximum values when RH is in the range 25–75%. Van Durme et al. [107] have also studied the effect of humidity on PPC removal of toluene. As for IPC, PPC is less efficient when RH increases. With Pd/Al<sub>2</sub>O<sub>3</sub> as PPC removal efficiencies are >90% and 37% at dry air and air with 74% RH (298 K), respectively. The negative humidity effect is mostly attributed to changing Van der Waals interactions.

In a recent study by Huang et al. [168], NTP has been combined with a photocatalyst located downstream. Experimental results indicate that catalytic ozonation plays a vital role in toluene decomposition. The dominant active species in the NTP-driven photocatalytic system are active oxygen species formed from ozone catalytic decomposition. The decomposition pathway of toluene



has been elucidated in subsequent work [188]. Detected byproducts for IPC removal of toluene with TiO<sub>2</sub>/Al<sub>2</sub>O<sub>3</sub>/nickel foam include benzene, benzaldehyde, formic acid and small amounts of acetic acid and 2-methylamylene.

Subrahmanyam et al. [134] modified a sintered metal fibre filter, which acts as inner electrode, with MnO<sub>x</sub> and CoO<sub>x</sub>. Fig. 13 shows the influence of this modification and energy density on the conversion of 100 ppm toluene. At an energy density of 235 J/L, nearly 100% conversion has been achieved with both MnO<sub>x</sub> and CoO<sub>x</sub>/SMF. Whereas SMF only shows 50% CO<sub>2</sub> selectivity, MnO<sub>x</sub>/SMF reaches 80% even at 235 J/L. Interestingly, no polymeric carbon deposits are detected. All the catalytic electrodes maintain the same activity during almost 3 h of toluene decomposition. This proves that the electrodes maintain their stability during VOC destruction.

Magureanu et al. [142] have tested MnPO<sub>4</sub>, Mn-APO-5 and Mn-SAPO-11 as PPC catalysts in an oven for temperatures up to 673 K. Even at low temperature, a remarkable synergetic effect has been observed while the catalysts alone are not active at that temperature level. The authors expect a further increase in the plasma-catalytic synergy by placing the catalyst in the discharge region, where short-lived species produced in the plasma will most likely contribute to oxidation on the catalyst surface.

### 3. Critical process parameters

Various process parameters determine the initial condition of the feeded gas stream. In the following section these parameters are discussed which are critical for an effective operation of both catalytic and non-catalytic NTP systems. For each parameter, the different influences on the removal performance of the configuration will be discussed and compared if possible.

#### 3.1. Temperature

In most cases, the NTP process removes VOCs more effectively as the process temperature increases. This is ascribed to an increased reaction rate of O and OH radicals with VOCs due to the endothermic behaviour of these reactions [53,127,189–195]. This is, however, only the case for VOCs that are primarily decomposed through radical reactions. When electron impact is thought to be the primary decomposition step (e.g. CCl<sub>4</sub>), no temperature dependence on the removal is observed because the electron density is not really influenced hereby [196,197]. However, in Ref. [198] CCl<sub>4</sub> destruction is greatly improved at high temperature. This can be explained by the fact that the maximum energy density is also significantly higher than in [196], which might lead to higher decomposition.

The improved removal rate and energy efficiency can also be explained by an increase in the reduced electric field ( $E/n$ ) with increasing temperatures. The reduced electric field, being the ratio of the electric field ( $E$ ) and the gas density ( $n$ ), is an important factor that determines the electron energy in the plasma. Since the gas density decreases as the gas temperature increases at constant pressure, NTP systems tend to operate at a higher reduced electric field [192,199].

When the catalyst is located downstream, NTP produced ozone can be decomposed by reaction with molecular oxygen in the gas phase:



The rate constant of this reaction is accelerated at elevated temperatures (5 times higher at 573 K compared to 373 K). However, the lifetime of the produced oxygen atoms in the gas phase is too short to react with VOCs adsorbed on the catalyst surface. At the same time, reactions at the catalyst surface between adsorbed oxygen atoms and VOCs are also accelerated. The net-result of these two competing effects is the most likely explanation for

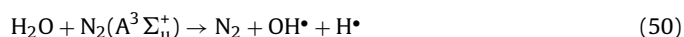
the different temperature dependencies found in literature: with increasing temperature, VOC decomposition efficiency can remain almost constant [142], can increase [149,153,180] or can decrease [127].

#### 3.2. Initial VOC concentration

Generally, the VOC concentration of actual industrial exhaust streams strongly varies. Therefore the effect of VOC concentration on the removal process has been abundantly studied. When the initial concentration rises, each VOC molecule shares fewer electrons and reactive plasma species. Consequently, numerous research papers have pointed out that higher initial VOC concentrations are detrimental for the removal efficiency in catalytic and non-catalytic NTP systems. Some papers also indicate that the characteristic energy [200–204] (i.e. the energy density needed to decompose 63% of the initial VOC concentration) and the energy yield [49,199,205] are an increasing function of the initial VOC concentration. For some halogenated carbons, the initial concentration barely seems to affect the decomposition efficiency. This is the case for HFC-134a [206], CFC-12 [207], HCFC-22 [208] and TCE [62]. This may be partly attributed to secondary decomposition induced by fragment ions and radicals produced by primary destruction steps [62]. Another plausible explanation may be that for these compounds the primary destruction by reactive plasma species is the rate-determining step, leading to similar decomposition efficiencies regardless of the initial concentration [208].

#### 3.3. Humidity level

The effect of humidity is of great interest for practical applications in industry since process gas consists of ambient air that usually contains water vapor at fluctuating concentrations. It appears that the effect of water vapor strongly depends on its concentration as well as on the type of the target VOC and the type of discharge. Water plays an important role in the plasma chemistry since it decomposes into OH and H radicals in a NTP environment as follows:



The oxidation power of OH is generally much stronger than those of other oxidants such as oxygen atoms and peroxy radicals.

The introduction of water vapor can induce changes in the electrical and physical properties of the discharge. The effect of water vapor has been mostly studied with (packed) DBD reactors. For this type of discharge, the presence of water vapor is known to reduce the total charge transferred in a microdischarge which ultimately decreases the volume of the reactive plasma zone [68]. The plasma characteristics of corona discharges are also affected by the presence of water vapor. At higher RH, lower currents are observed for a given voltage [83]. This is attributed to a higher probability of the plasma attachment processes resulting in a reduced OH production [209]. Water also has an adverse effect on VOC removal due to its electronegative characteristic which limits the electron density and quenches activated chemical species [82].

The effect of humidity has been tested for several VOCs. It seems that the addition of water negatively influences the properties of the discharge irrespective of the VOC chemical structure. However, the enhanced production of OH caused by higher water vapor content competes with the latter effect, depending on the VOC chemical structure [210]. The influence on the removal process is designated as an enhancement, a suppression or a neutral effect depending on the chemical structure of the target VOC. Table 10



**Table 10**  
Influence of humidity on VOC removal with NTP.

Target VOC	Plasma type	Influence	References
Acetylene	DBD	Suppression	[166]
Benzene	Packed DBD	Suppression	[66]
Benzene	DBD	Suppression	[69]
Benzene	Packed DBD	Suppression	[283]
Butane	DBD	Suppression	[213]
Chloroform	Gliding arc	Suppression	[284]
Dichloromethane	Packed DBD	Suppression	[205]
Formaldehyde	DBD	Neutral	[194]
Methane	DBD	Enhancement	[247]
Methanol	Packed DBD	Neutral	[205]
Propane	DBD	Neutral	[193]
TCE	DBD	Suppression	[213]
TCE	Surface discharge	Suppression	[285]
TCE	SPCP <sup>a</sup>	Neutral	[286]
Tetrachloromethane	Packed DBD	Suppression	[216]
Tetrachloromethane	Gliding arc	Suppression	[284]
Toluene	Corona	Enhancement	[169]
Toluene	Packed DBD	Neutral	[205]
Toluene	Pulsed corona	Suppression	[244]
Toluene	Gliding arc	Neutral	[199]
Toluene	Surface discharge	Neutral	[140]
1,1,1-Trichloroethane	DBD	Suppression	[287]
p-Xylene	DBD	Enhancement	[192]

<sup>a</sup> Surface discharge induced plasma chemical processing.

gives an overview of research results concerning the effect of humidity on the decomposition efficiency in various plasma reactors. Some studies have shown that an optimal water vapor content exists for achieving a maximum VOC removal efficiency. Interestingly, this optimum is around 20% RH for both TCE [211] and toluene [82,83]. Furthermore, addition of water counteracts the formation of ozone due to consumption of O(<sup>1</sup>D) (reaction (51)) which is the most important origin of ozone formation [179]. It has also been shown that water vapor decreases the formation of CO and enhances the selectivity towards CO<sub>2</sub> [166,212,213].

In case of a PPC system, catalytic ozonation will play a minor role due to the inhibition of ozone formation by humidity. Secondly, the catalyst surface can be covered with layers of H<sub>2</sub>O preventing the adsorption of ozone and VOCs and consequently minimizing direct catalyst/VOC intermolecular interactions [107,122,186,214]. In this context, the morphology and chemical composition of the catalyst are important factors that influence the interactions with H<sub>2</sub>O. Therefore, it is desirable to choose a catalyst that is less susceptible to H<sub>2</sub>O adsorption. Finally, increased humidity can poison catalytic active sites and lower the catalysts activity [122,214].

#### 3.4. Oxygen content

Similar to the presence of water vapor, the oxygen content in the gas stream affects the discharge performance and plays a very important role in the occurring chemical reactions. A small increase in oxygen concentration generally leads to an enhanced generation of reactive oxygen radicals, resulting in a higher removal efficiency. However, due to its electronegative character, higher oxygen concentrations tend to trigger electron attachment reactions. Consequently, this limits the electron density and changes the electron energy distribution functions [215,216]. Also, oxygen and oxygen radicals are able to consume reactive species such as excited nitrogen molecules and nitrogen atoms, which are otherwise used for destroying VOCs [217–219]. Collectively, the phenomena described above ensure the existence of an optimal oxygen content for VOC removal with NTP (Table 11). It appears that the optimal oxygen content ranges between 1% and 5%. For practical application in industrial waste gas treatment, it is, however, in most cases difficult to control the oxygen content to this

**Table 11**  
Optimal oxygen content for VOC removal with NTP.

Target VOC	Optimal O <sub>2</sub> content (%)	References
Acetaldehyde	3–5	[215]
Benzene	0.2	[73]
Benzene	3–5	[75]
Carbon tetrafluoride	1	[288]
Dichloromethane	1–3	[243]
2-Heptanone	2–3	[200]
HCFC-22	0.5	[208]
HFC-134a	0.5	[206]
Methylbromide	2	[289]
TCE	2	[290]
Toluene	3–5	[75]
Toluene	2	[102]
Trichloromethane	0.5	[217]
p-Xylene	5	[192]

level because process gas depends on its industrial environment and in a lot of situations it consists of ambient air.

Similar effects are observed for IPC systems. Additionally, direct reactions between oxygen radicals and VOC molecules adsorbed on the catalyst surface add to the positive effect of a moderate O<sub>2</sub> addition to N<sub>2</sub> [220]. However, in [75], several catalysts (TiO<sub>2</sub>, γ-Al<sub>2</sub>O<sub>3</sub>, zeolites) have been tested at varying oxygen content for the removal of toluene and benzene with a cycled system of removal and adsorption. For all catalysts tested, the removal efficiency increased with oxygen content ranging from 0% to 100%. Operation at higher oxygen content is also able to reduce the formation of N<sub>2</sub>O and NO<sub>2</sub>.

As for the influence of the oxygen content on the performance of PPC configurations, no studies were found in literature.

#### 3.5. Gas flow rate

The gas flow rate applied in laboratory experiments generally ranges from 0.1 L/min to 10 L/min. The effect of decreasing the gas flow rate logically implies an increase in residence time of the VOC in the system. Hence, the collision probability for electron-impact reactions and for reactions between VOCs and plasma generated radicals and metastables is enhanced which increases the decomposition efficiency.

When the NTP system is combined with a catalyst, the same argumentation can be made. In that case, the increased probability of surface reactions is beneficial for the removal process.

In the interest of practical operation, some groups have studied multistage NTP reactors with the aim to increase the residence time without decreasing the gas flow rate [116,221–224].

## 4. Future trends

The extensive literature review regarding NTP and plasma-catalytic decomposition of VOCs demonstrates that there are still challenges that have to be addressed in future work.

For plasma-alone systems, incomplete oxidation of VOCs leads to the formation of various intermediate and unwanted byproducts. Although for certain compounds decomposition mechanisms are proposed, there is still need to expand the knowledge on plasma-chemical kinetics. The derived information about e.g. the distribution of byproducts can be very useful to choose an appropriate catalyst or to enhance existing catalytic formulations in order to increase the efficiency of the hybrid system.

In the case of plasma-catalytic systems, synergistic effects on the overall removal efficiency are often observed. The mechanisms that contribute to this synergy are thoroughly investigated and different elucidations are proposed in literature often showing discrepancies between them. Therefore, better understanding of

which mechanisms have the most important contributions and which chemical species play a dominant role in the decomposition of VOCs is still of great interest. From this point of view, development of well-designed instruments specialized in *in situ* measurements is crucial.

The research of plasma material interactions for VOC treatment is recently looking at the opportunity to regenerate VOC saturated surfaces with the aid of NTP systems [225–227]. This process of alternate adsorption and desorption can convert flue gases with a large flow rate and low VOC concentration into that with a low flow rate and high concentration. Further developments could yield an economical VOC removal process for small- and medium-sized facilities that emit diluted VOC waste gases. Therefore, further progress on this subject is suspected in the nearby future.

## References

- P.S. Monks, C. Granier, S. Fuzzi, A. Stohl, M.L. Williams, H. Akimoto, M. Amann, A. Baklanov, U. Baltensperger, I. Bey, N. Blake, R.S. Blake, K. Carslaw, O.R. Cooper, F. Dentener, D. Fowler, E. Fragkou, G.J. Frost, S. Generoso, P. Ginoux, V. Grewet, A. Guenther, H.C. Hansson, S. Hennew, J. Hjorth, A. Hofzumahaus, H. Huntrieser, I.S.A. Isaksen, M.E. Jenkin, J. Kaiser, M. Kanakidou, Z. Klimont, M. Kulmala, P. Laj, M.G. Lawrence, J.D. Lee, C. Lioussis, M. Maione, G. McFiggans, A. Metzger, A. Mieville, N. Moussiopoulos, J.J. Orlando, C.D. O'Dowd, P.I. Palmer, D.D. Parrish, A. Petzold, U. Platt, U. Pöschl, A.S.H. Prevot, C.E. Reeves, S. Reimann, Y. Rudich, K. Sellegri, R. Steinbrecher, D. Simpson, H. ten Brink, J. Theloke, G.R. van der Werf, R. Vautard, V. Vestreng, C. Vlachokostas, R. von Glasow, Atmospheric composition change—global and regional air quality, *Atmospheric Environment* 43 (2009) 5268–5350.
- R. Atkinson, Atmospheric chemistry of VOCs and NO<sub>x</sub>, *Atmospheric Environment* 34 (2000) 2063–2101.
- J.R. Odum, T.P.W. Jungkamp, R.J. Griffin, H.J.L. Forstner, R.C. Flagan, J.H. Seinfeld, Aromatics, reformulated gasoline, and atmospheric organic aerosol formation, *Environmental Science & Technology* 31 (1997) 1890–1897.
- R.A. Larson, E.J. Weber, *Reaction Mechanisms in Environmental Organic Chemistry*, Lewis Publishers, 2010.
- J. Chorria, M. Jaroniec, M. Kloske, Ordered siliceous and carbonaceous nanomaterials in environmental protection, *Ochrona Srodowiska* 29 (2007) 3–12.
- W.B. Li, H. Gong, Recent progress in the removal of volatile organic compounds by catalytic combustion, *Acta Physico-Chimica Sinica* 26 (2010) 885–894.
- A. Kumar, J. Dewulf, H. Van Langenhove, Membrane-based biological waste gas treatment, *Chemical Engineering Journal* 136 (2008) 82–91.
- S. Mudliar, B. Giri, K. Padoley, D. Satpute, R. Dixit, P. Bhatt, R. Pandey, A. Juwarkar, A. Vaidya, Bioreactors for treatment of VOCs and odours—a review, *Journal of Environmental Management* 91 (2010) 1039–1054.
- K. Demeestere, J. Dewulf, H. Van Langenhove, Heterogeneous photocatalysis as an advanced oxidation process for the abatement of chlorinated, monocyclic aromatic and sulfurous volatile organic compounds in air: state of the art, *Critical Reviews in Environmental Science and Technology* 37 (2007) 489–538.
- F.I. Khan, A.K. Ghoshal, Removal of volatile organic compounds from polluted air, *Journal of Loss Prevention in the Process Industries* 13 (2000) 527–545.
- T. Yamamoto, K. Ramanathan, P.A. Lawless, D.S. Ensor, J.R. Newsome, N. Plaks, G.H. Ramsey, Control of volatile organic compounds by an AC energized ferroelectric pellet reactor and a pulsed corona reactor, *IEEE Transactions on Industry Applications* 28 (1992) 528–534.
- C.M. Nunez, G.H. Ramsey, W.H. Ponder, J.H. Abbott, L.E. Hamel, P.H. Kariher, Corona destruction: an innovative control technology for VOCs and air toxics, *Air and Waste* 43 (1993) 242–247.
- H.H. Kim, Nonthermal plasma processing for air-pollution control: a historical review, current issues, and future prospects, *Plasma Processes and Polymers* 1 (2004) 91–110.
- J.Y. Park, J.G. Jung, J.S. Kim, G.H. Rim, K.S. Kim, Effect of nonthermal plasma reactor for CF<sub>4</sub> decomposition, *IEEE Transactions on Plasma Science* 31 (2003) 1349–1354.
- T. Yamamoto, B.S. Rajanikanth, M. Okubo, T. Kuroki, M. Nishino, Performance evaluation of nonthermal plasma reactors for NO oxidation in diesel engine exhaust gas treatment, *IEEE Transactions on Industry Applications* 39 (2003) 1608–1613.
- H.B. Ma, P. Chen, M.L. Zhang, X.Y. Lin, R. Ruan, Study of SO<sub>2</sub> removal using non-thermal plasma induced by dielectric barrier discharge (DBD), *Plasma Chemistry and Plasma Processing* 22 (2002) 239–254.
- Y.H. Song, S.J. Kim, K.I. Choi, T. Yamamoto, Effects of adsorption and temperature on a nonthermal plasma process for removing VOCs, *Journal of Electrostatics* 55 (2002) 189–201.
- U. Roland, F. Holzer, E.D. Kopinke, Combination of non-thermal plasma and heterogeneous catalysis for oxidation of volatile organic compounds Part 2. Ozone decomposition and deactivation of gamma-Al<sub>2</sub>O<sub>3</sub>, *Applied Catalysis B: Environmental* 58 (2005) 217–226.
- C. Subrahmanyam, Catalytic non-thermal plasma reactor for total oxidation of volatile organic compounds, *Indian Journal of Chemistry Section A: Inorganic Bio-Inorganic Physical Theoretical & Analytical Chemistry* 48 (2009) 1062–1068.
- T. Zhu, J. Li, W.J. Liang, Y.Q. Jin, Synergistic effect of catalyst for oxidation removal of toluene, *Journal of Hazardous Materials* 165 (2009) 1258–1260.
- A. Mizuno, Industrial applications of atmospheric non-thermal plasma in environmental remediation, *Plasma Physics and Controlled Fusion* 49 (2007) A1–A15.
- J.S. Chang, P.A. Lawless, T. Yamamoto, Corona discharge processes, *IEEE Transactions on Plasma Science* 19 (1991) 1152–1166.
- A. Fridman, A. Chirokov, A. Gutsol, Non-thermal atmospheric pressure discharges, *Journal of Physics D: Applied Physics* 38 (2005) R1–R24.
- U. Kogelschatz, Dielectric-barrier discharges: their history, discharge physics, and industrial applications, *Plasma Chemistry and Plasma Processing* 23 (2003) 1–46.
- V. Nehra, A. Kumar, H.K. Dwivedi, Atmospheric non-thermal plasma sources, *International Journal of Engineering* 2 (2008) 53–68.
- R. Hackam, H. Akiyama, Air pollution control by electrical discharges, *IEEE Transactions on Dielectrics and Electrical Insulation* 7 (2000) 654–683.
- T. Yamamoto, S. Futamura, Nonthermal plasma processing for controlling volatile organic compounds, *Combustion Science and Technology* 133 (1998) 117–133.
- B. Eliasson, M. Hirth, U. Kogelschatz, Ozone synthesis from oxygen in dielectric barrier discharges, *Journal of Physics D: Applied Physics* 20 (1987) 1421–1437.
- G.J. Pietsch, Peculiarities of dielectric barrier discharges, *Contributions to Plasma Physics* 41 (2001) 620–628.
- S. Masuda, S. Hosokawa, X.L. Tu, K. Sakakibara, S. Kitoh, S. Sakai, Destruction of gaseous-pollutants by surface-induced plasma chemical process (SpCs), *IEEE Transactions on Industry Applications* 29 (1993) 781–786.
- S. Masuda, S. Hosokawa, X. Tu, Z. Wang, Novel plasma chemical technologies—Pcp and Spcp for control of gaseous-pollutants and air toxics, *Journal of Electrostatics* 34 (1995) 415–438.
- K. Urashima, J.S. Chang, T. Ito, Reduction of NO<sub>x</sub> from combustion flue gases by superimposed barrier discharge plasma reactors, *IEEE Transactions on Industry Applications* 33 (1997) 879–886.
- R. McAdams, Prospects for non-thermal atmospheric plasmas for pollution abatement, *Journal of Physics D: Applied Physics* 34 (2001) 2810–2821.
- J. Jarrige, P. Vervisch, Decomposition of three volatile organic compounds by nanosecond pulsed corona discharge: study of by-product formation and influence of high voltage pulse parameters, *Journal of Applied Physics* 99 (2006).
- M. Nifuku, M. Horvath, J. Bodnar, G.Y. Zhang, T. Tanaka, E. Kiss, G. Woy-narovich, H. Katoh, A study on the decomposition of volatile organic compounds by pulse corona, *Journal of Electrostatics* 40–1 (1997) 687–692.
- E.H.W.M. Smulders, B.E.J.M. van Heesch, S.S.V.B. van Paasen, Pulsed power corona discharges for air pollution control, *IEEE Transactions on Plasma Science* 26 (1998) 1476–1484.
- K.F. Shang, Y. Wu, J. Li, G.F. Li, D. Li, N.H. Wang, Reduction of NO<sub>x</sub>/SO<sub>2</sub> by wire-plate type pulsed discharge reactor with pulsed corona radical shower, *Plasma Chemistry and Plasma Processing* 26 (2006) 443–454.
- Y. Shi, J. Ruan, X. Wang, W. Li, T. Tan, Decomposition of mixed malodorants in a wire-plate pulse corona reactor, *Environmental Science & Technology* 39 (2005) 6786–6791.
- W.J. Liang, J. Li, Y.Q. Jin, Abatement of toluene from gas streams via ferroelectric packed bed dielectric barrier discharge plasma, *Journal of Hazardous Materials* 170 (2009) 633–638.
- A. Ogata, N. Shintani, K. Mizuno, S. Kushiya, T. Yamamoto, Decomposition of benzene using a nonthermal plasma reactor packed with ferroelectric pellets, *IEEE Transactions on Industry Applications* 35 (1999) 753–759.
- U. Roland, F. Holzer, F.D. Kopinke, Improved oxidation of air pollutants in a non-thermal plasma, *Catalysis Today* 73 (2002) 315–323.
- S. Okazaki, M. Kogoma, M. Uehara, Y. Kimura, Appearance of stable glow-discharge in air, argon, oxygen and nitrogen at atmospheric-pressure using a 50-Hz source, *Journal of Physics D: Applied Physics* 26 (1993) 889–892.
- Y. Akishev, A. Deryugin, V. Karal'nik, I. Kochetov, A. Napartovich, N. Trushkin, Numerical simulation and experimental study of an atmospheric pressure direct-current glow discharge, *Plasma Physics Reports* 20 (1994) 511–524.
- D. Trunec, A. Brablec, F. Stastny, Experimental study of atmospheric pressure glow discharge, *Contributions to Plasma Physics* 38 (1998) 435–445.
- E.E. Kunhardt, Generation of large-volume, atmospheric-pressure, nonequilibrium plasmas, *IEEE Transactions on Plasma Science* 28 (2000) 189–200.
- Y.S. Akishev, M.E. Grushin, I.V. Kochetov, A.P. Napartovich, M.V. Pan'kin, N.I. Trushkin, Transition of a multipin negative corona in atmospheric air to a glow discharge, *Plasma Physics Reports* 26 (2000) 157–163.
- Y. Akishev, O. Goossens, T. Callebaut, C. Leys, A. Napartovich, N. Trushkin, The influence of electrode geometry and gas flow on corona-to-glow and glow-to-spark threshold currents in air, *Journal of Physics D: Applied Physics* 34 (2001) 2875–2882.
- T. Callebaut, I. Kochetov, Y. Akishev, A. Napartovich, C. Leys, Numerical simulation and experimental study of the corona and glow regime of a negative pin-to-plate discharge in flowing ambient air, *Plasma Sources Science & Technology* 13 (2004) 245–250.
- R. Vertrieest, R. Morent, J. Dewulf, C. Leys, H. Van Langenhove, Multi-pin-to-plate atmospheric glow discharge for the removal of volatile organic

- compounds in waste air, *Plasma Sources Science & Technology* 12 (2003) 412–416.
- [50] D.S. Antao, D.A. Staack, A. Fridman, B. Farouk, Atmospheric pressure DC corona discharges: operating regimes and potential applications, *Plasma Sources Science & Technology* 18 (2009) 035016 (035011 pp.).
- [51] D. Evans, L.A. Rosocha, G.K. Anderson, J.J. Coogan, M.J. Kushner, Plasma remediation of trichloroethylene in silent discharge plasmas, *Journal of Applied Physics* 74 (1993) 5378–5386.
- [52] M.J. Kirkpatrick, W.C. Finney, B.R. Locke, Chlorinated organic compound removal by gas phase pulsed streamer corona electrical discharge with reticulated vitreous carbon electrodes, *Plasmas and Polymers* 8 (2003) 165–177.
- [53] M.C. Hsiao, B.T. Merritt, B.M. Penetrante, G.E. Vogtlin, P.H. Wallman, Plasma-assisted decomposition of methanol and trichloroethylene in atmospheric-pressure air streams by electrical-discharge processing, *Journal of Applied Physics* 78 (1995) 3451–3456.
- [54] L. Prager, H. Langguth, S. Rummel, R. Mehnert, Electron-beam degradation of chlorinated hydrocarbons in air, *Radiation Physics and Chemistry* 46 (1995) 1137–1142.
- [55] T. Hakoda, S. Hashimoto, Y. Fujiyama, A. Mizuno, Decomposition mechanism for electron beam irradiation of vaporized trichloroethylene-air mixtures, *Journal of Physical Chemistry A* 104 (2000) 59–66.
- [56] T. Hakoda, G. Zhang, S. Hashimoto, Decomposition of chloroethenes in electron beam irradiation, *Radiation Physics and Chemistry* 54 (1999) 541–546.
- [57] S.A. Vitale, K. Hadidi, D.R. Cohn, P. Falko, The effect of a carbon-carbon double bond on electron beam-generated plasma decomposition of trichloroethylene and 1,1,1-trichloroethane, *Plasma Chemistry and Plasma Processing* 17 (1997) 59–78.
- [58] E. Sanhueza, I.C. Hisatsune, J. Heicklen, Oxidation of haloethylenes, *Chemical Reviews* 76 (1976) 801–826.
- [59] G. Huybrech, L. Meyers, Gas-phase chlorine-photosensitized oxidation of trichloroethylene, *Transactions of the Faraday Society* 62 (1966) 2191.
- [60] L. Bertrand, J.A. Franklin, P. Goldfing, G. Huybrech, Point of attack of a chlorine atom on trichloroethylene, *Journal of Physical Chemistry* 72 (1968) 3926.
- [61] B.M. Penetrante, M.C. Hsiao, J.N. Bardsley, B.T. Merritt, G.E. Vogtlin, A. Kuthi, C.P. Burkhardt, J.R. Bayless, Identification of mechanisms for decomposition of air pollutants by non-thermal plasma processing, *Plasma Sources Science & Technology* 6 (1997) 251–259.
- [62] S. Futamura, T. Yamamoto, Byproduct identification and mechanism determination in plasma chemical decomposition of trichloroethylene, *IEEE Transactions on Industry Applications* 33 (1997) 447–453.
- [63] K. Urashima, J.S. Chang, Removal of volatile organic compounds from air streams and industrial flue gases by non-thermal plasma technology, *IEEE Transactions on Dielectrics and Electrical Insulation* 7 (2000) 602–614.
- [64] J.S. Chang, K. Urashima, T. Ito, Mechanism of non-thermal plasma treatment of volatile organic compounds in dry air, in: D.W. Tedder, F.G. Pohland (Eds.), *Emerging Technologies in Hazardous Waste Management*, ACS Press, Atlanta, 1994, pp. 203–206.
- [65] S.B. Han, T. Oda, Decomposition mechanism of trichloroethylene based on by-product distribution in the hybrid barrier discharge plasma process, *Plasma Sources Science & Technology* 16 (2007) 413–421.
- [66] A. Ogata, N. Shintani, K. Yamanouchi, K. Mizuno, S. Kushiyama, T. Yamamoto, Effect of water vapor on benzene decomposition using a nonthermal-discharge plasma reactor, *Plasma Chemistry and Plasma Processing* 20 (2000) 453–467.
- [67] H.H. Kim, H. Kobara, A. Ogata, S. Futamura, Comparative assessment of different nonthermal plasma reactors on energy efficiency and aerosol formation from the decomposition of gas-phase benzene, *IEEE Transactions on Industry Applications* 41 (2005) 206–214.
- [68] Z. Falkenstein, J.J. Coogan, Microdischarge behaviour in the silent discharge of nitrogen-oxygen and water-air mixtures, *Journal of Physics D: Applied Physics* 30 (1997) 817–825.
- [69] M.P. Cal, M. Schluep, Destruction of benzene with non-thermal plasma in dielectric barrier discharge reactors, *Environmental Progress* 20 (2001) 151–156.
- [70] B.Y. Lee, S.H. Park, S.C. Lee, M. Kang, S.J. Choung, Decomposition of benzene by using a discharge plasma-photocatalyst hybrid system, *Catalysis Today* 93–5 (2004) 769–776.
- [71] Z.L. Ye, Y.N. Zhang, P. Li, L.Y. Yang, R.X. Zhang, H.Q. Hou, Feasibility of destruction of gaseous benzene with dielectric barrier discharge, *Journal of Hazardous Materials* 156 (2008) 356–364.
- [72] C.Q. Jiang, A.A.H. Mohamed, R.H. Stark, J.H. Yuan, K.H. Schoenbach, Removal of volatile organic compounds in atmospheric pressure air by means of direct current glow discharges, *IEEE Transactions on Plasma Science* 33 (2005) 1416–1425.
- [73] K. Satoh, T. Matsuzawa, H. Itoh, Decomposition of benzene in a corona discharge at atmospheric pressure, *Thin Solid Films* 516 (2008) 4423–4429.
- [74] N. Goto, H. Kurimoto, S. Kudo, Y. Wanatabe, Decomposition of benzene by barrier discharge in  $N_2$  at low concentrations of  $O_2$ , *IEEE Transactions on Fundamentals and Materials* 123 (2003) 900–906.
- [75] H.H. Kim, A. Ogata, S. Futamura, Oxygen partial pressure-dependent behavior of various catalysts for the total oxidation of VOCs using cycled system of adsorption and oxygen plasma, *Applied Catalysis B: Environmental* 79 (2008) 356–367.
- [76] M.F. Golde, Reactions of  $N_2(A^3\Sigma-U^+)$ , *International Journal of Chemical Kinetics* 20 (1988) 75–92.
- [77] G.R. Dey, A. Sharma, K.K. Pushpa, T.N. Das, Variable products in dielectric-barrier discharge assisted benzene oxidation, *Journal of Hazardous Materials* 178 (2010) 693–698.
- [78] H. Kohno, A.A. Berezin, J.S. Chang, M. Tamura, T. Yamamoto, A. Shibuya, S. Hondo, Destruction of volatile organic compounds used in a semiconductor industry by a capillary tube discharge reactor, *IEEE Transactions on Industry Applications* 34 (1998) 953–966.
- [79] W. Mista, R. Kacprzyk, Decomposition of toluene using non-thermal plasma reactor at room temperature, *Catalysis Today* 137 (2008) 345–349.
- [80] Z. Machala, E. Marode, M. Morvová, P. Lukáč, DC glow discharge in atmospheric air as a source for volatile organic compounds abatement, *Plasma Processes and Polymers* 2 (2005) 152–161.
- [81] S. Ogner, S. Cavadias, J. Amouroux, Aromatic VOC removal by formation of microparticles in pure nitrogen discharge, *Plasma Processes and Polymers* 4 (2007) 528–536.
- [82] Y.F. Guo, D.Q. Ye, K.F. Chen, Y.F. Tian, Humidity effect on toluene decomposition in a wire-plate dielectric barrier discharge reactor, *Plasma Chemistry and Plasma Processing* 26 (2006) 237–249.
- [83] J. Van Durme, J. Dewulf, W. Szymans, C. Leys, H. Van Langenhove, Abatement and degradation pathways of toluene in indoor air by positive corona discharge, *Chemosphere* 68 (2007) 1821–1829.
- [84] M. Schiorlin, E. Marotta, M. Rea, C. Paradisi, Comparison of toluene removal in air at atmospheric conditions by different corona discharges, *Environmental Science & Technology* 43 (2009) 9386–9392.
- [85] F. Holzer, U. Roland, F.D. Kopinke, Combination of non-thermal plasma and heterogeneous catalysis for oxidation of volatile organic compounds Part 1. Accessibility of the intra-particle volume, *Applied Catalysis B: Environmental* 38 (2002) 163–181.
- [86] H.L. Chen, H.M. Lee, S.H. Chen, M.B. Chang, S.J. Yu, S.N. Li, Removal of volatile organic compounds by single-stage and two-stage plasma catalysis systems: a review of the performance enhancement mechanisms, current status, and suitable applications, *Environmental Science & Technology* 43 (2009) 2216–2227.
- [87] X. Chen, J. Rozak, J.C. Lin, S.L. Suib, J. Hayashi, H. Matsumoto, Oxidative decomposition of chlorinated hydrocarbons by glow discharge in PACT (plasma and catalyst integrated technologies) reactors, *Applied Catalysis A: General* 219 (2001) 25–31.
- [88] M.B. Chang, H.M. Lee, Abatement of perfluorocarbons with combined plasma catalysis in atmospheric-pressure environment, *Catalysis Today* 89 (2004) 109–115.
- [89] S.J. Yu, M.B. Chang, Oxidative conversion of PFC via plasma processing with dielectric barrier discharges, *Plasma Chemistry and Plasma Processing* 21 (2001) 311–327.
- [90] M.A. Malik, Y. Minamitani, K.H. Schoenbach, Comparison of catalytic activity of aluminum oxide and silica gel for decomposition of volatile organic compounds (VOCs) in a plasma-catalytic reactor, *IEEE Transactions on Plasma Science* 33 (2005) 50–56.
- [91] F. Holzer, F.D. Kopinke, U. Roland, Influence of ferroelectric materials and catalysts on the performance of non-thermal plasma (NTP) for the removal of air pollutants, *Plasma Chemistry and Plasma Processing* 25 (2005) 595–611.
- [92] H.L. Chen, H.M. Lee, S.H. Chen, M.B. Chang, Review of packed-bed plasma reactor for ozone generation and air pollution control, *Industrial & Engineering Chemistry Research* 47 (2008) 2122–2130.
- [93] J.O. Chae, V. Demidiouk, M. Yeulash, I.C. Choi, T.G. Jung, Experimental study for indoor air control by plasma-catalyst hybrid system, *IEEE Transactions on Plasma Science* 32 (2004) 493–497.
- [94] J.G. Wang, C.J. Liu, Y.P. Zhang, K.L. Yu, X.L. Zhu, F. He, Partial oxidation of methane to syngas over glow discharge plasma treated Ni-Fe/ $Al_2O_3$  catalyst, *Catalysis Today* 89 (2004) 183–191.
- [95] Z.H. Li, S.X. Tian, H.T. Wang, H.B. Tian, Plasma treatment of Ni catalyst via a corona discharge, *Journal of Molecular Catalysis A: Chemical* 211 (2004) 149–153.
- [96] X.L. Zhu, P.P. Huo, Y.P. Zhang, C.J. Liu, Characterization of argon glow discharge plasma reduced Pt/ $Al_2O_3$  catalyst, *Industrial & Engineering Chemistry Research* 45 (2006) 8604–8609.
- [97] C.J. Liu, J.J. Zou, K.L. Yu, D.G. Cheng, Y. Han, J. Zhan, C. Ratanawanate, B.W.L. Jang, Plasma application for more environmentally friendly catalyst preparation, *Pure and Applied Chemistry* 78 (2006) 1227–1238.
- [98] C. Ratanawanate, M. Macias, B.W.L. Jang, Promotion effect of the nonthermal RF plasma treatment on Ni/ $Al_2O_3$  for benzene hydrogenation, *Industrial & Engineering Chemistry Research* 44 (2005) 9868–9874.
- [99] Y.R. Zhu, Z.H. Li, Y.B. Zhou, J. Lv, H.T. Wang, Plasma treatment of Ni and Pt catalysts for partial oxidation of methane, *Reaction Kinetics and Catalysis Letters* 87 (2005) 33–41.
- [100] Y.F. Guo, D.Q. Ye, K.F. Chen, J.C. He, W.L. Chen, Toluene decomposition using a wire-plate dielectric barrier discharge reactor with manganese oxide catalyst in situ, *Journal of Molecular Catalysis A: Chemical* 245 (2006) 93–100.
- [101] Y.P. Zhang, P.S. Ma, X.L. Zhu, C.J. Liu, Y.T. Shen, A novel plasma-treated Pt/ $NazSM-5$  catalyst for NO reduction by methane, *Catalysis Communications* 5 (2004) 35–39.
- [102] Y.F. Guo, D.Q. Ye, K.F. Chen, J.C. He, Toluene removal by a DBD-type plasma combined with metal oxides catalysts supported by nickel foam, *Catalysis Today* 126 (2007) 328–337.

- [103] A.E. Wallis, J.C. Whitehead, K. Zhang, Plasma-assisted catalysis for the destruction of CFC-12 in atmospheric pressure gas streams using TiO<sub>2</sub>, *Catalysis Letters* 113 (2007) 29–33.
- [104] A.S. Pribytkov, G.N. Baeva, N.S. Telegina, A.L. Tarasov, A.Y. Stakheev, A.V. Tel'nov, V.N. Golubeva, Effect of electron irradiation on the catalytic properties of supported Pd catalysts, *Kinetics and Catalysis* 47 (2006) 765–769.
- [105] A.E. Wallis, J.C. Whitehead, K. Zhang, The removal of dichloromethane from atmospheric pressure nitrogen gas streams using plasma-assisted catalysis, *Applied Catalysis B: Environmental* 74 (2007) 111–116.
- [106] A. Rousseau, O. Guaitella, J. Ropcke, L.V. Gatilova, Y.A. Tolmachev, Combination of a pulsed microwave plasma with a catalyst for acetylene oxidation, *Applied Physics Letters* 85 (2004) 2199–2201.
- [107] J. Van Durme, J. Dewulf, K. Demeestere, C. Leys, H. Van Langenhove, Post-plasma catalytic technology for the removal of toluene from indoor air: effect of humidity, *Applied Catalysis B: Environmental* 87 (2009) 78–83.
- [108] B. Lu, X. Zhang, X. Yu, T. Feng, S. Yao, Catalytic oxidation of benzene using DBD corona discharges, *Journal of Hazardous Materials* 137 (2006) 633–637.
- [109] H.H. Kim, A. Ogata, S. Futamura, Effect of different catalysts on the decomposition of VOCs using flow-type plasma-driven catalysis, *IEEE Transactions on Plasma Science* 34 (2006) 984–995.
- [110] T. Sano, N. Negishi, E. Sakai, S. Matsuzawa, Contributions of photocatalytic/catalytic activities of TiO<sub>2</sub> and gamma-Al<sub>2</sub>O<sub>3</sub> in nonthermal plasma on oxidation of acetaldehyde and CO, *Journal of Molecular Catalysis A: Chemical* 245 (2006) 235–241.
- [111] H.B. Huang, D.Q. Ye, M.L. Fu, F. Da Feng, Contribution of UV light to the decomposition of toluene in dielectric barrier discharge plasma/photocatalysis system, *Plasma Chemistry and Plasma Processing* 27 (2007) 577–588.
- [112] H.H. Kim, S.M. Oh, A. Ogata, S. Futamura, Decomposition of gas-phase benzene using plasma-driven catalyst (PDC) reactor packed with Ag/TiO<sub>2</sub> catalyst, *Applied Catalysis B: Environmental* 56 (2005) 213–220.
- [113] M. Kang, B.J. Kim, S.M. Cho, C.H. Chung, B.W. Kim, G.Y. Han, K.J. Yoon, Decomposition of toluene using an atmospheric pressure plasma/TiO<sub>2</sub> catalytic system, *Journal of Molecular Catalysis A: Chemical* 180 (2002) 125–132.
- [114] M. Kang, Y.R. Ko, M.K. Jeon, S.C. Lee, S.J. Choung, J.Y. Park, S. Klim, S.H. Choi, Characterization of Bi/TiO<sub>2</sub> nanometer sized particle synthesized by solvothermal method and CH<sub>3</sub>CHO decomposition in a plasma-photocatalytic system, *Journal of Photochemistry and Photobiology A: Chemistry* 173 (2005) 128–136.
- [115] C. Subrahmanyam, M. Magureanu, D. Laub, A. Renken, L. Kiwi-Minsker, Non-thermal plasma abatement of trichloroethylene enhanced by photocatalysis, *Journal of Physical Chemistry C* 111 (2007) 4315–4318.
- [116] S. Chavadej, K. Saktrakool, P. Rangsunvigit, L.L. Lobban, T. Sreethawong, Oxidation of ethylene by a multistage corona discharge system in the absence and presence of Pt/TiO<sub>2</sub>, *Chemical Engineering Journal* 132 (2007) 345–353.
- [117] A. Ogata, H.H. Kim, S.M. Oh, S. Futamura, Evidence for direct activation of solid surface by plasma discharge on CFC decomposition, *Thin Solid Films* 506 (2006) 373–377.
- [118] R. Morent, J. Dewulf, N. Steenhaut, C. Leys, H. Van Langenhove, Hybrid plasma-catalyst system for the removal of trichloroethylene in air, *Journal of Advanced Oxidation Technologies* 9 (2006) 53–58.
- [119] K. Takaki, K. Urashima, J.S. Chang, Ferro-electric pellet shape effect on C2F6 removal by a packed-bed-type nonthermal plasma reactor, *IEEE Transactions on Plasma Science* 32 (2004) 2175–2183.
- [120] K. Urashima, K.G. Kostov, J.S. Chang, Y. Okayasu, T. Iwaizumi, K. Yoshimura, T. Kato, Removal of C2F6 from a semiconductor process flue gas by a ferroelectric packed-bed barrier discharge reactor with an adsorber, *IEEE Transactions on Industry Applications* 37 (2001) 1456–1463.
- [121] C. Leys, D. Neiryneck, R. Morent, E. Temmerman, DC-excited cold atmospheric pressure plasmas, *Czechoslovak Journal of Physics* 56 (2006) B896–B902.
- [122] H.B. Huang, D.Q. Ye, Combination of photocatalysis downstream the non-thermal plasma reactor for oxidation of gas-phase toluene, *Journal of Hazardous Materials* 171 (2009) 535–541.
- [123] H.B. Huang, D.Q. Ye, X.J. Guan, The simultaneous catalytic removal of VOCs and O-3 in a post-plasma, *Catalysis Today* 139 (2008) 43–48.
- [124] N. Blin-Simiand, P. Tardiveau, A. Risacher, F. Jorand, S. Pasquiers, Removal of 2-heptanone by dielectric barrier discharges—the effect of a catalyst support, *Plasma Processes and Polymers* 2 (2005) 256–262.
- [125] K. Krawczyk, B. Ulejczyk, H.K. Song, A. Lamenta, B. Paluch, K. Schmidt-Szalowski, Plasma-catalytic reactor for decomposition of chlorinated hydrocarbons, *Plasma Chemistry and Plasma Processing* 29 (2009) 27–41.
- [126] V. Demidiouk, J.O. Chae, Decomposition of volatile organic compounds in plasma-catalytic system, *IEEE Transactions on Plasma Science* 33 (2005) 157–161.
- [127] K. Hayashi, H. Yasui, M. Tanaka, S. Futamura, S. Kurita, K. Aoyagi, Temperature dependence of toluene decomposition behavior in the discharge-catalyst hybrid reactor, *IEEE Transactions on Industry Applications* 45 (2009) 1553–1558.
- [128] K. Hensel, S. Katsura, A. Mizuno, DC microdischarges inside porous ceramics, *IEEE Transactions on Plasma Science* 33 (2005) 574–575.
- [129] S. Futamura, H. Einaga, H. Kabashima, L.Y. Hwan, Synergistic effect of silent discharge plasma and catalysts on benzene decomposition, *Catalysis Today* 89 (2004) 89–95.
- [130] M.J. Kirkpatrick, W.C. Finney, B.R. Locke, Plasma-catalyst interactions in the treatment of volatile organic compounds and NO<sub>x</sub> with pulsed corona discharge and reticulated vitreous carbon Pt/Rh-coated electrodes, *Catalysis Today* 89 (2004) 117–126.
- [131] C. Subrahmanyam, A. Renken, L. Kiwi-Minsker, Novel catalytic non-thermal plasma reactor for the abatement of VOCs, *Chemical Engineering Journal* 134 (2007) 78–83.
- [132] C. Subrahmanyam, A. Renken, L. Kiwi-Minsker, Novel catalytic dielectric barrier discharge reactor for gas-phase abatement of isopropanol, *Plasma Chemistry and Plasma Processing* 27 (2007) 13–22.
- [133] M. Magureanu, N.B. Mandache, V.I. Parvulescu, C. Subrahmanyam, A. Renken, L. Kiwi-Minsker, Improved performance of non-thermal plasma reactor during decomposition of trichloroethylene: optimization of the reactor geometry and introduction of catalytic electrode, *Applied Catalysis B: Environmental* 74 (2007) 270–277.
- [134] C. Subrahmanyam, A. Renken, L. Kiwi-Minsker, Catalytic non-thermal plasma reactor for abatement of toluene, *Chemical Engineering Journal* 160 (2010) 677–682.
- [135] X. Chen, J. Rozak, J.C. Lin, S.L. Suib, Y. Hayashi, H. Matsumoto, Oxidative decomposition of chlorinated hydrocarbons by glow discharge in PACT (plasma and catalyst integrated technologies) reactors, *Applied Catalysis A: General* 219 (2001) 25–31.
- [136] A. Ogata, K. Yamanouchi, K. Mizuno, S. Kushiyama, T. Yamamoto, Oxidation of dilute benzene in an alumina hybrid plasma reactor at atmospheric pressure, *Plasma Chemistry and Plasma Processing* 19 (1999) 383–394.
- [137] A. Ogata, K. Yamanouchi, K. Mizuno, S. Kushiyama, T. Yamamoto, Decomposition of benzene using alumina-hybrid and catalyst-hybrid plasma reactors, *IEEE Transactions on Industry Applications* 35 (1999) 1289–1295.
- [138] T. Oda, K. Yamaji, Dilute trichloroethylene decomposition in air by using non-thermal plasma—catalyst effect, *Journal of Advanced Oxidation Technologies* 6 (2003) 93–99.
- [139] A. Ogata, D. Ito, K. Mizuno, S. Kushiyama, T. Yamamoto, Removal of dilute benzene using a zeolite-hybrid plasma reactor, *IEEE Transactions on Industry Applications* 37 (2001) 959–964.
- [140] S.M. Oh, H.H. Kim, A. Ogata, H. Einaga, S. Futamura, D.W. Park, Effect of zeolite in surface discharge plasma on the decomposition of toluene, *Catalysis Letters* 99 (2005) 101–104.
- [141] S.M. Oh, H.H. Kim, H. Einaga, A. Ogata, S. Futamura, D.W. Park, Zeolite-combined plasma reactor for decomposition of toluene, *Thin Solid Films* 506 (2006) 418–422.
- [142] M. Magureanu, N.B. Mandache, P. Eloy, E.M. Gaigneaux, V.I. Parvulescu, Plasma-assisted catalysis for volatile organic compounds abatement, *Applied Catalysis B: Environmental* 61 (2005) 12–20.
- [143] T. Oda, T. Takahashi, S. Kohzuma, Decomposition of dilute trichloroethylene by using nonthermal plasma processing-frequency and catalyst effects, *IEEE Transactions on Industry Applications* 37 (2001) 965–970.
- [144] A.E. Wallis, J.C. Whitehead, K. Zhang, The removal of dichloromethane from atmospheric pressure air streams using plasma-assisted catalysis, *Applied Catalysis B: Environmental* 72 (2007) 282–288.
- [145] A. Ogata, H. Einaga, H. Kabashima, S. Futamura, S. Kushiyama, H.H. Kim, Effective combination of nonthermal plasma and catalysts for decomposition of benzene in air, *Applied Catalysis B: Environmental* 46 (2003) 87–95.
- [146] H. Grossmannova, D. Neiryneck, C. Leys, Atmospheric discharge combined with Cu-Mn/Al<sub>2</sub>O<sub>3</sub> catalyst unit for the removal of toluene, *Czechoslovak Journal of Physics* 56 (2006) B1156–B1161.
- [147] A. Vandenbroucke, R. Morent, N. De Geyter, M.T. Nguyen Dinh, J.M. Giraudon, J.F. Lamonier, C. Leys, Plasma-catalytic decomposition of TCE, *International Journal of Plasma Environmental Science and Technology* 4 (2010) 135–138.
- [148] P. Da Costa, R. Marques, S. Da Costa, Plasma catalytic oxidation of methane on alumina-supported noble metal catalysts, *Applied Catalysis B: Environmental* 84 (2008) 214–222.
- [149] T. Blackburn, V. Demidiouk, S.L. Hill, J.C. Whitehead, The effect of temperature on the plasma-catalytic destruction of propane and propene: a comparison with thermal catalysis, *Plasma Chemistry and Plasma Processing* 29 (2009) 411–419.
- [150] T. Yamamoto, K. Mizuno, I. Tamori, A. Ogata, M. Nifuku, M. Michalska, G. Prieto, Catalysis-assisted plasma technology for carbon tetrachloride destruction, *IEEE Transactions on Industry Applications* 32 (1996) 100–105.
- [151] C.L. Chang, H.L. Bai, S.J. Lu, Destruction of styrene in an air stream by packed dielectric barrier discharge reactors, *Plasma Chemistry and Plasma Processing* 25 (2005) 641–657.
- [152] M.B. Chang, H.M. Lee, Abatement of perfluorocarbons with combined plasma-catalysis in atmospheric pressure environment, *Catalysis Today* 89 (2004) 109–115.
- [153] V. Demidiouk, J.C. Whitehead, Influence of temperature on gas-phase toluene decomposition in plasma-catalytic system, *Plasma Chemistry and Plasma Processing* 27 (2007) 85–94.
- [154] V. Demidiouk, S.I. Moon, J.O. Chae, D.Y. Lee, Application of a plasma-catalytic system for decomposition of volatile organic compounds, *Journal of the Korean Physical Society* 42 (2003) S966–S970.
- [155] C.L. Chang, T.S. Lin, Elimination of carbon monoxide in the gas streams by dielectric barrier discharge systems with Mn catalyst, *Plasma Chemistry and Plasma Processing* 25 (2005) 387–401.
- [156] H.L. Chen, H.M. Lee, L.C. Cheng, M.B. Chang, S.J. Yu, S.N. Li, Influence of non-thermal plasma reactor type on CF<sub>4</sub> and SF<sub>6</sub> abatements, *IEEE Transactions on Plasma Science* 36 (2008) 509–515.

- [157] J. Jarrige, P. Vervisch, Plasma-enhanced catalysis of propane and isopropyl alcohol at ambient temperature on a MnO<sub>2</sub>-based catalyst, *Applied Catalysis B: Environmental* 90 (2009) 74–82.
- [158] X. Fan, T.L. Zhu, M.Y. Wang, X.M. Li, Removal of low concentration BTX in air using a combined plasma catalysis system, *Chemosphere* 75 (2009) 1301–1306.
- [159] T. Hakoda, K. Matsumoto, A. Mizuno, K. Hirota, Role of metals loaded on a TiO<sub>2</sub> surface in the oxidation of xylene in air using an electron beam irradiation/catalytic process, *Applied Catalysis A: General* 357 (2009) 244–249.
- [160] A.S. Besov, A.V. Vorontsov, Acceleration of acetone destruction process under synergistic action of photocatalytic oxidation and barrier discharge, *Plasma Chemistry and Plasma Processing* 27 (2007) 624–634.
- [161] T. Oda, K. Yamaji, T. Takahashi, Decomposition of dilute trichloroethylene by nonthermal plasma processing—gas flow rate, catalyst, and ozone effect, *IEEE Transactions on Industry Applications* 40 (2004) 430–436.
- [162] T. Oda, T. Takahashi, K. Yamaji, Nonthermal plasma processing for dilute VOCs decomposition, *IEEE Transactions on Industry Applications* 38 (2002) 873–878.
- [163] D.W. Park, S.H. Yoon, G.J. Kim, H. Sekiguchi, The effect of catalyst on the decomposition of dilute benzene using dielectric barrier discharge, *Journal of Industrial and Engineering Chemistry* 8 (2002) 393–398.
- [164] R.B. Sun, Z.G. Xi, F.H. Chao, W. Zhang, H.S. Zhang, D.F. Yang, Decomposition of low-concentration gas-phase toluene using plasma-driven photocatalyst reactor, *Atmospheric Environment* 41 (2007) 6853–6859.
- [165] O. Guaitella, F. Thevenet, E. Puzenat, C. Guillard, A. Rousseau, C<sub>2</sub>H<sub>2</sub> oxidation by plasma/TiO<sub>2</sub> combination: influence of the porosity, and photocatalytic mechanisms under plasma exposure, *Applied Catalysis B: Environmental* 80 (2008) 296–305.
- [166] F. Thevenet, O. Guaitella, E. Puzenat, C. Guillard, A. Rousseau, Influence of water vapour on plasma/photocatalytic oxidation efficiency of acetylene, *Applied Catalysis B: Environmental* 84 (2008) 813–820.
- [167] C.L. Chang, T.S. Lin, Decomposition of toluene and acetone in packed dielectric barrier discharge reactors, *Plasma Chemistry and Plasma Processing* 25 (2005) 227–243.
- [168] H.B. Huang, D.Q. Ye, D.Y.C. Leung, Removal of toluene using UV-irradiated and nonthermal plasma-driven photocatalyst system, *Journal of Environmental Engineering: ASCE* 136 (2010) 1231–1236.
- [169] M. Kogoma, Y. Miki, K. Tanaka, K. Takahashi, Highly efficient VOC decomposition using a complex system (OH Radical, Ozone-UV, and TiO<sub>2</sub>), *Plasma Processes and Polymers* 3 (2006) 727–733.
- [170] T. Oda, T. Takahashi, K. Yamaji, TCE decomposition by the non-thermal plasma process concerning ozone effect, *IEEE Transaction on Industrial Applications* 40 (2004) 1249–1256.
- [171] S.B. Han, T. Oda, R. Ono, Improvement of the energy efficiency in the decomposition of dilute trichloroethylene by the barrier discharge plasma process, *IEEE Transactions on Industry Applications* 41 (2005) 1343–1349.
- [172] M. Magureanu, N.B. Mandache, J.C. Hu, R. Richards, M. Florea, V.I. Parvulescu, Plasma-assisted catalysis total oxidation of trichloroethylene over gold nanoparticles embedded in SBA-15 catalysts, *Applied Catalysis B: Environmental* 76 (2007) 275–281.
- [173] A.M. Vandenbroucke, R. Morent, N. De Geyter, C. Leys, Decomposition of trichloroethylene with plasma-catalysis: a review, *Journal of Advanced Oxidation Technologies* 14 (2011) 165–173.
- [174] H.H. Kim, Y.H. Lee, A. Ogata, S. Futamura, Plasma-driven catalyst processing packed with photocatalyst for gas-phase benzene decomposition, *Catalysis Communications* 4 (2003) 347–351.
- [175] H.H. Kim, A. Ogata, S. Futamura, Y.H. Lee, Decomposition of gas-phase benzene using hybrid systems of a non-thermal plasma and catalysts, *Journal of the Korean Physical Society* 44 (2004) 1163–1167.
- [176] H.H. Kim, A. Ogata, S. Futamura, Atmospheric plasma-driven catalysis for the low temperature decomposition of dilute aromatic compounds, *Journal of Physics D: Applied Physics* 38 (2005) 1292–1300.
- [177] H.H. Kim, S.M. Oh, A. Ogata, S. Futamura, Decomposition of benzene using Ag/TiO<sub>2</sub> packed plasma-driven catalyst reactor: influence of electrode configuration and Ag-loading amount, *Catalysis Letters* 96 (2004) 189–194.
- [178] H.Y. Fan, C. Shi, X.S. Li, D.Z. Zhao, Y. Xu, High-efficiency plasma catalytic removal of dilute benzene from air, *Journal of Physics D: Applied Physics* 42 (2009) 225105.
- [179] T. Zhu, J. Li, Y. Jin, Y. Liang, G. Ma, Decomposition of benzene by non-thermal plasma processing: photocatalyst and ozone effect, *International Journal of Environmental Science and Technology* 5 (2008) 375–384.
- [180] A.M. Harling, V. Demidyuk, S.J. Fischer, J.C. Whitehead, Plasma-catalysis destruction of aromatics for environmental clean-up: effect of temperature and configuration, *Applied Catalysis B: Environmental* 82 (2008) 180–189.
- [181] M.A. Malik, X.Z. Jiang, Catalyst assisted destruction of trichloroethylene and toluene in corona discharges, *Journal of Environmental Sciences* 12 (2000) 7–11.
- [182] D.A. Li, D. Yakushiji, S. Kanazawa, T. Ohkubo, Y. Nomoto, Decomposition of toluene by streamer corona discharge with catalyst, *Journal of Electrostatics* 55 (2002) 311–319.
- [183] Y.F. Guo, X. Liao, J.H. He, W. Ou, D.Q. Ye, Effect of manganese oxide catalyst on the dielectric barrier discharge decomposition of toluene, *Catalysis Today* 153 (2010) 176–183.
- [184] Y.F. Guo, X.B. Liao, D.Q. Ye, *Journal of Environmental Science: China* 20 (2008) 1429.
- [185] X.B. Liao, Y.F. Guo, J.H. He, W.J. Ou, D.Q. Ye, Hydroxyl radicals formation in dielectric barrier discharge during decomposition of toluene, *Plasma Chemistry and Plasma Processing* 30 (2010) 841–853.
- [186] J. Van Durme, J. Dewulf, W. Sysmans, C. Leys, H. Van Langenhove, Efficient toluene abatement in indoor air by a plasma catalytic hybrid system, *Applied Catalysis B: Environmental* 74 (2007) 161–169.
- [187] H.B. Huang, D.Q. Ye, D.Y.C. Leung, Plasma-driven catalysis process for toluene abatement: effect of water vapor, *IEEE Transactions on Plasma Science* 39 (2011) 576–580.
- [188] H. Huang, D.Q. Ye, D.Y.C. Leung, F. Feng, X.J. Guan, Byproducts and pathways of toluene destruction via plasma-catalysis, *Journal of Molecular Catalysis A: Chemical* 336 (2011) 87–93.
- [189] B.M. Penetrante, M.C. Hsiao, J.N. Bardsley, B.T. Merritt, G.E. Vogtlin, A. Kuthi, C.P. Burkhart, J.R. Bayless, Decomposition of methylene chloride by electron beam and pulsed corona processing, *Physics Letters A* 235 (1997) 76–82.
- [190] V. Demidyuk, S.L. Hill, J.C. Whitehead, Enhancement of the destruction of propane in a low-temperature plasma by the addition of unsaturated hydrocarbons: experiment and modeling, *Journal of Physical Chemistry A* 112 (2008) 7862–7867.
- [191] N. Blin-Simiand, S. Pasquiers, F. Jorand, C. Postel, J.R. Vacher, Removal of formaldehyde in nitrogen and in dry air by a DBD: importance of temperature and role of nitrogen metastable states, *Journal of Physics D: Applied Physics* 42 (2009).
- [192] H.M. Lee, M.B. Chang, Abatement of gas-phase p-xylene via dielectric barrier discharges, *Plasma Chemistry and Plasma Processing* 23 (2003) 541–558.
- [193] O. Aubry, J.M. Cormier, Improvement of the diluted propane efficiency treatment using a non-thermal plasma, *Plasma Chemistry and Plasma Processing* 29 (2009) 13–25.
- [194] D.G. Storch, M.J. Kushner, Destruction mechanisms for formaldehyde in atmospheric-pressure low-temperature plasmas, *Journal of Applied Physics* 73 (1993) 51–55.
- [195] J. Li, S.P. Bai, X.C. Shi, S.L. Han, X.M. Zhu, W.C. Chen, Y.K. Pu, Effects of temperature on benzene oxidation in dielectric barrier discharges, *Plasma Chemistry and Plasma Processing* 28 (2008) 39–48.
- [196] B.M. Penetrante, M.C. Hsiao, J.N. Bardsley, B.T. Merritt, G.E. Vogtlin, P.H. Wallman, Electron beam and pulsed corona processing of volatile organic compounds in gas streams, *Pure and Applied Chemistry* 68 (1996) 1083–1087.
- [197] A.M. Harling, H.H. Kim, S. Futamura, J.C. Whitehead, Temperature dependence of plasma-catalysis using a nonthermal, atmospheric pressure packed bed; the destruction of benzene and toluene, *Journal of Physical Chemistry C* 111 (2007) 5090–5095.
- [198] L.W. Huang, K. Nakajyo, T. Hari, S. Ozawa, H. Matsuda, Decomposition of carbon tetrachloride by a pulsed corona reactor incorporated with in situ absorption, *Industrial & Engineering Chemistry Research* 40 (2001) 5481–5486.
- [199] C.M. Du, J.H. Yan, B. Cheron, Decomposition of toluene in a gliding arc discharge plasma reactor, *Plasma Sources Science & Technology* 16 (2007) 791–797.
- [200] A.S. Chipper, N. Blin-Simiand, M. Heninger, H. Mestdagh, P. Boissel, F. Jorand, J. Lemaire, J. Leprovost, S. Pasquiers, G. Popa, C. Postel, Detailed characterization of 2-heptanone conversion by dielectric barrier discharge in N<sub>2</sub> and N<sub>2</sub>/O<sub>2</sub> mixtures, *Journal of Physical Chemistry A* 114 (2010) 397–407.
- [201] N. Blin-Simiand, F. Jorand, L. Magne, S. Pasquiers, C. Postel, J.R. Vacher, Plasma reactivity and plasma-surface interactions during treatment of toluene by a dielectric barrier discharge, *Plasma Chemistry and Plasma Processing* 28 (2008) 429–466.
- [202] S. Delagrang, L. Pinard, J.M. Tatibouet, Combination of a non-thermal plasma and a catalyst for toluene removal from air: manganese based oxide catalysts, *Applied Catalysis B: Environmental* 68 (2006) 92–98.
- [203] J.H. Byeon, J.H. Park, Y.S. Jo, K.Y. Yoon, J. Hwang, Removal of gaseous toluene and submicron aerosol particles using a dielectric barrier discharge reactor, *Journal of Hazardous Materials* 175 (2010) 417–422.
- [204] L.A. Rosocha, R.A. Korzekwa, Advanced oxidation and reduction processes in the gas phase using non-thermal plasmas, *Journal of Advanced Oxidation Technologies* 4 (1999) 247–264.
- [205] S. Futamura, M. Sugasawa, Additive effect on energy efficiency and byproduct distribution in VOC decomposition with nonthermal plasma, *IEEE Transactions on Industry Applications* 44 (2008) 40–45.
- [206] Y.S. Mok, V. Demidyuk, J.C. Whitehead, Decomposition of hydrofluorocarbons in a dielectric-packed plasma reactor, *Journal of Physical Chemistry A* 112 (2008) 6586–6591.
- [207] H.C. Kang, Decomposition of chlorofluorocarbon by non-thermal plasma, *Journal of Industrial and Engineering Chemistry* 8 (2002) 488–492.
- [208] J.H. Oh, Y.S. Mok, S.B. Lee, Destruction of HCFC-22 and distribution of byproducts in a nonthermal plasma reactor packed with dielectric pellets, *Journal of Korean Physical Society* 54 (2009) 1539–1546.
- [209] L. Fouad, S. Elhazek, Effect of humidity on positive corona discharge in a 3-electrode system, *Journal of Electrostatics* 35 (1995) 21–30.
- [210] M. Sugasawa, T. Terasawa, S. Futamura, Additive effect of water on the decomposition of VOCs in nonthermal plasma, *IEEE Transactions on Industry Applications* 46 (2010) 1692–1698.
- [211] Y. Nakagawa, H. Fujisawa, R. Ono, T. Oda, Dilute trichloroethylene decomposition by using high pressure non-thermal plasma-humidity effects, in: 2010 IEEE Industry Applications Society Annual Meeting, 2010.



- [212] A. Ogata, D. Ito, K. Mizuno, S. Kushiyama, A. Gal, T. Yamamoto, Effect of coexisting components on aromatic decomposition in a packed-bed plasma reactor, *Applied Catalysis A: General* 236 (2002) 9–15.
- [213] S. Futamura, A.H. Zhang, T. Yamamoto, The dependence of nonthermal plasma behavior of VOCs on their chemical structures, *Journal of Electrostatics* 42 (1997) 51–62.
- [214] H. Einaga, T. Ibusuki, S. Futamura, Performance evaluation of a hybrid system comprising silent discharge plasma and manganese oxide catalysts for benzene decomposition, *IEEE Transactions on Industry Applications* 37 (2001) 1476–1482.
- [215] H.M. Lee, M.B. Chang, Gas-phase removal of acetaldehyde via packed-bed dielectric barrier discharge reactor, *Plasma Chemistry and Plasma Processing* 21 (2001) 329–343.
- [216] R.G. Tonkyn, S.E. Barlow, T.M. Orlando, Destruction of carbon tetrachloride in a dielectric barrier/packed-bed corona reactor, *Journal of Applied Physics* 80 (1996) 4877–4886.
- [217] Y.S. Mok, S.B. Lee, J.H. Oh, K.S. Ra, B.H. Sung, Abatement of trichloromethane by using nonthermal plasma reactors, *Plasma Chemistry and Plasma Processing* 28 (2008) 663–676.
- [218] A. Ogata, K. Mizuno, S. Kushiyama, T. Yamamoto, Methane decomposition in a barium titanate packed-bed nonthermal plasma reactor, *Plasma Chemistry and Plasma Processing* 18 (1998) 363–373.
- [219] K.J. Pringle, J.C. Whitehead, J.J. Wilman, J.H. Wu, The chemistry of methane remediation by a non-thermal atmospheric pressure plasma, *Plasma Chemistry and Plasma Processing* 24 (2004) 421–434.
- [220] H.X. Ding, A.M. Zhu, F.G. Lu, Y. Xu, J. Zhang, X.F. Yang, Low-temperature plasma-catalytic oxidation of formaldehyde in atmospheric pressure gas streams, *Journal of Physics D: Applied Physics* 39 (2006) 3603–3608.
- [221] A.M. Harling, D.J. Glover, J.C. Whitehead, K. Zhang, Industrial scale destruction of environmental pollutants using a novel plasma reactor, *Industrial & Engineering Chemistry Research* 47 (2008) 5856–5860.
- [222] S. Chavadej, W. Kiatubolpaiboon, P. Rangsunvigit, T. Sreethawong, A combined multistage corona discharge and catalytic system for gaseous benzene removal, *Journal of Molecular Catalysis A: Chemical* 263 (2007) 128–136.
- [223] Y. Shi, J.J. Ruan, X. Wang, W. Li, T.E. Tan, Evaluation of multiple corona reactor modes and the application in odor removal, *Plasma Chemistry and Plasma Processing* 26 (2006) 187–196.
- [224] A.M. Harling, D.J. Glover, J.C. Whitehead, K. Zhang, Novel method for enhancing the destruction of environmental pollutants by the combination of multiple plasma discharges, *Environmental Science & Technology* 42 (2008) 4546–4550.
- [225] T. Kuroki, T. Fujioka, R. Kawabata, M. Okubo, T. Yamamoto, Regeneration of honeycomb zeolite by nonthermal plasma desorption of toluene, *IEEE Transactions on Industry Applications* 45 (2009) 10–15.
- [226] H.H. Kim, S. Tsubota, M. Date, A. Ogata, S. Futamura, Catalyst regeneration and activity enhancement of Au/TiO<sub>2</sub> by atmospheric pressure nonthermal plasma, *Applied Catalysis A: General* 329 (2007) 93–98.
- [227] T. Kuroki, T. Fujioka, M. Okubo, T. Yamamoto, Toluene concentration using honeycomb nonthermal plasma desorption, *Thin Solid Films* 515 (2007) 4272–4277.
- [228] J. Van Durme, J. Dewulf, C. Leys, H. Van Langenhove, Combining non-thermal plasma with heterogeneous catalysis in waste gas treatment: a review, *Applied Catalysis B: Environmental* 78 (2008) 324–333.
- [229] M. Magureau, N.B. Mandache, V.I. Parvulescu, Chlorinated organic compounds decomposition in a dielectric barrier discharge, *Plasma Chemistry and Plasma Processing* 27 (2007) 679–690.
- [230] Z.L. Ye, Y. Shen, R.X. Zhang, H.Q. Hou, Destruction of benzene in an air stream by the outer combined plasma photolysis method, *Journal of Physics D: Applied Physics* 41 (2008).
- [231] A. Ogata, K. Miyamae, K. Mizuno, S. Kushiyama, M. Tezuka, Decomposition of benzene in air in a plasma reactor: effect of reactor type and operating conditions, *Plasma Chemistry and Plasma Processing* 22 (2002) 537–552.
- [232] C.H. Lin, H. Bai, Energy effectiveness of nonthermal plasma reactors for toluene vapor destruction, *Journal of Environmental Engineering* 127 (2001) 648–654.
- [233] A.D. Koutsospyros, S.M. Yin, C. Christodoulatos, K. Becker, Plasmochemical degradation of volatile organic compounds (VOC) in a capillary discharge plasma reactor, *IEEE Transactions on Plasma Science* 33 (2005) 42–49.
- [234] K. Faungnawakij, N. Sano, D. Yamamoto, T. Kanki, T. Charinpanitkul, W. Tanthapanichakoon, Removal of acetaldehyde in air using a wetted-wall corona discharge reactor, *Chemical Engineering Journal* 103 (2004) 115–122.
- [235] T. Oda, A. Kumada, K. Tanaka, T. Takahashi, S. Masuda, Low-temperature atmospheric-pressure discharge plasma processing for volatile organic compounds, *Journal of Electrostatics* 35 (1995) 93–101.
- [236] T. Oda, R. Yamashita, I. Haga, T. Takahashi, S. Masuda, Decomposition of gaseous organic contaminants by surface discharge induced plasma chemical processing SPCP, *IEEE Transactions on Industry Applications* 32 (1996) 118–124.
- [237] R. Rudolph, K.P. Francke, H. Miessner, Concentration dependence of VOC decomposition by dielectric barrier discharges, *Plasma Chemistry and Plasma Processing* 22 (2002) 401–412.
- [238] H.C. Wang, D. Li, Y. Wu, J. Li, G.F. Li, Removal of four kinds of volatile organic compounds mixture in air using silent discharge reactor driven by bipolar pulsed power, *Journal of Electrostatics* 67 (2009) 547–553.
- [239] M.N. Lyulyukin, A.S. Besov, A.V. Vorontsov, The influence of corona electrodes thickness on the efficiency of plasmachemical oxidation of acetone, *Plasma Chemistry and Plasma Processing* 31 (2011) 23–39.
- [240] M.G. Sobacchi, A.V. Saveliev, A.A. Fridman, A.F. Gutsol, L.A. Kennedy, Experimental assessment of pulsed corona discharge for treatment of VOC emissions, *Plasma Chemistry and Plasma Processing* 23 (2003) 347–370.
- [241] J. Hoard, T.J. Wallington, R.L. Bretz, A. Malkin, R. Dorai, M.J. Kushner, Importance of O(P-3) atoms and OH radicals in hydrocarbon oxidation during the nonthermal plasma treatment of diesel exhaust inferred using relative-rate methods, *International Journal of Chemical Kinetics* 35 (2003) 231–238.
- [242] A. Rousseau, O. Guaitella, L. Gatilova, M. Hannemann, J. Ropcke, Measurement of the C<sub>2</sub>H<sub>2</sub> destruction kinetics by infrared laser absorption spectroscopy in a pulsed low pressure dc discharge, *Journal of Physics D: Applied Physics* 40 (2007) 2018–2025.
- [243] C. Fitzsimons, F. Ismail, J.C. Whitehead, J.J. Wilman, The chemistry of dichloromethane destruction in atmospheric-pressure gas streams by a dielectric packed-bed plasma reactor, *Journal of Physical Chemistry A* 104 (2000) 6032–6038.
- [244] R.A. Korzekwa, M.G. Grothaus, R.K. Hutcherson, R.A. Roush, R. Brown, Destruction of hazardous air pollutants using a fast rise time pulsed corona reactor, *Review of Scientific Instruments* 69 (1998) 1886–1892.
- [245] E. Marotta, G. Scorrano, C. Paradisi, Ionic reactions of chlorinated volatile organic compounds in air plasma at atmospheric pressure, *Plasma Processes and Polymers* 2 (2005) 209–217.
- [246] M. Sugawara, G. Annadurai, S. Futamura, Reaction behavior of toluene-dichloromethane mixture in nonthermal plasma, *IEEE Transactions on Industry Applications* 45 (2009) 1499–1505.
- [247] A. Mfopara, M.J. Kirkpatrick, E. Odic, Dilute methane treatment by atmospheric pressure dielectric barrier discharge: effects of water vapor, *Plasma Chemistry and Plasma Processing* 29 (2009) 91–102.
- [248] M. Derakhshesh, J. Abedi, H. Hassanzadeh, Mechanism of methanol decomposition by non-thermal plasma, *Journal of Electrostatics* 68 (2010) 424–428.
- [249] R. Taranto, D. Frochot, P. Pichat, Combining cold plasma and TiO<sub>2</sub> photocatalysis to purify gaseous effluents: a preliminary study using methanol-contaminated air, *Industrial & Engineering Chemistry Research* 46 (2007) 7611–7614.
- [250] T. Sato, M. Kambe, H. Nishiyama, Analysis of a methanol decomposition process by a nonthermal plasma flow, *JSME International Journal Series B: Fluids and Thermal Engineering* 48 (2005) 432–439.
- [251] S.L. Hill, J.C. Whitehead, K. Zhang, Plasma processing of propane at hyper-atmospheric pressure: experiment and modelling, *Plasma Processes and Polymers* 4 (2007) 710–718.
- [252] S.L. Hill, H.H. Kim, S. Futamura, J.C. Whitehead, The destruction of atmospheric pressure propane and propene using a surface discharge plasma reactor, *Journal of Physical Chemistry A* 112 (2008) 3953–3958.
- [253] N. Moreau, S. Pasquiers, N. Blin-Simiand, L. Magne, F. Jorand, C. Postel, J.R. Vacher, Propane dissociation in a non-thermal high-pressure nitrogen plasma, *Journal of Physics D: Applied Physics* 43 (2010), -.
- [254] Y.S. Mok, C.M. Nam, M.H. Cho, I.S. Nam, Decomposition of volatile organic compounds and nitric oxide by nonthermal plasma discharge processes, *IEEE Transactions on Plasma Science* 30 (2002) 408–416.
- [255] I. Orlandini, U. Riedel, Oxidation of propene and the formation of methyl nitrate in non-thermal plasma discharges, *Catalysis Today* 89 (2004) 83–88.
- [256] G.K. Anderson, H. Snyder, J. Coogan, Oxidation of styrene in a silent discharge plasma, *Plasma Chemistry and Plasma Processing* 19 (1999) 131–151.
- [257] A. Ostapczuk, A.G. Chmielewski, V. Honkonen, J. Ruuskanen, J. Tarhanen, B. Svarfvar, Preliminary test in decomposition of styrene by electron beam treatment, *Radiation Physics and Chemistry* 56 (1999) 369–371.
- [258] B.M. Penetrante, M.C. Hsiao, J.N. Bardsley, B.T. Merritt, G.E. Vogtlin, P.H. Wallman, A. Kuthi, C.P. Burkhardt, J.R. Bayless, Electron-beam and pulsed corona processing of carbon-tetrachloride in atmospheric-pressure gas streams, *Physics Letters A* 209 (1995) 69–77.
- [259] A. Lamenta, S. Jodzis, K. Krawczyk, K. Schmidt-Szalowski, Carbon tetrachloride decomposition in spark discharge plasma, *Polish Journal of Chemistry* 83 (2009) 169–174.
- [260] S.J. Rubio, M.C. Quintero, A. Rodero, Application of microwave air plasma in the destruction of trichloroethylene and carbon tetrachloride at atmospheric pressure, *Journal of Hazardous Materials* 186 (2011) 820–826.
- [261] H. Kohno, M. Tamura, S. Honda, A. Shibuya, T. Yamamoto, A.A. Berezin, J.S. Chang, Generation of aerosol particles in the process of xylene and TCE decomposition from air streams by a ferroelectric packed-bed barrier discharge reactor, *Journal of Aerosol Science* 28 (1997) S413–S414.
- [262] T. Zhu, J. Li, Y.Q. Jin, Y.H. Liang, G.D. Ma, Gaseous phase benzene decomposition by non-thermal plasma coupled with nano titania catalyst, *International Journal of Environmental Science and Technology* 6 (2009) 141–148.
- [263] J.Y. Ban, Y.H. Son, M. Kang, S.J. Chung, Highly concentrated toluene decomposition on the dielectric barrier discharge (DBD) plasma-photocatalytic hybrid system with Mn-Ti-incorporated mesoporous silicate photocatalyst (Mn-Ti-MPS), *Applied Surface Science* 253 (2006) 535–542.
- [264] M. Magureau, N.B. Mandache, E. Gaigneaux, C. Paun, V.I. Parvulescu, Toluene oxidation in a plasma-catalytic system, *Journal of Applied Physics* 99 (2006).
- [265] A.M. Harling, D.J. Glover, J.C. Whitehead, K. Zhang, The role of ozone in the plasma-catalytic destruction of environmental pollutants, *Applied Catalysis B: Environmental* 90 (2009) 157–161.

- [266] V. Demidiouk, S.I. Moon, J.O. Chae, Toluene and butyl acetate removal from air by plasma–catalytic system, *Catalysis Communications* 4 (2003) 51–56.
- [267] A. Mizuno, Y. Kisanuki, M. Noguchi, S. Katsura, S.H. Lee, U.K. Hong, S.Y. Shin, J.H. Kang, Indoor air cleaning using a pulsed discharge plasma, *IEEE Transactions on Industry Applications* 35 (1999) 1284–1288.
- [268] T. Ohshima, T. Kondo, N. Kitajima, M. Sato, Adsorption and plasma decomposition of gaseous acetaldehyde on fibrous activated carbon, *IEEE Transactions on Industry Applications* 46 (2010) 23–28.
- [269] A. Rousseau, O. Guaitella, L. Gatilova, F. Thevenet, C. Guillard, J. Ropcke, G.D. Stancu, Photocatalyst activation in a pulsed low pressure discharge, *Applied Physics Letters* 87 (2005).
- [270] A.M. Harling, A.E. Wallis, J.C. Whitehead, The effect of temperature on the removal of DCM using non-thermal, atmospheric-pressure plasma-assisted catalysis, *Plasma Processes and Polymers* 4 (2007) 463–470.
- [271] A. Ogata, K. Saito, H.H. Kim, M. Sugawara, H. Aritani, H. Einaga, Performance of an ozone decomposition catalyst in hybrid plasma reactors for volatile organic compound removal, *Plasma Chemistry and Plasma Processing* 30 (2010) 33–42.
- [272] H.X. Ding, A.M. Zhu, X.F. Yang, C.H. Li, Y. Xu, Removal of formaldehyde from gas streams via packed-bed dielectric barrier discharge plasmas, *Journal of Physics D: Applied Physics* 38 (2005) 4160–4167.
- [273] R. Marques, S. Da Costa, P. Da Costa, Plasma-assisted catalytic oxidation of methane—on the influence of plasma energy deposition and feed composition, *Applied Catalysis B: Environmental* 82 (2008) 50–57.
- [274] J. Kim, B. Han, Y. Kim, J.H. Lee, C.R. Park, J.C. Kim, J.C. Kim, K.J. Kim, Removal of VOCs by hybrid electron beam reactor with catalyst bed, *Radiation Physics and Chemistry* 71 (2004) 429–432.
- [275] K.J. Kim, J.C. Kim, J.Y. Kim, Y. Sunwoo, Development of hybrid technology using E-beam and catalyst for aromatic VOCs control, *Radiation Physics and Chemistry* 73 (2005) 85–90.
- [276] T. Hakoda, A. Shimada, A. Kimura, M. Taguchi, Y. Sugo, K. Arak, E.B. Dally, K. Hirota, An electron-beam irradiation/catalytic oxidation system for purification of aromatic hydrocarbons/air mixture under practical gas-flow condition, *Industrial & Engineering Chemistry Research* 49 (2010) 5517–5522.
- [277] T. Hakoda, K. Matsumoto, A. Shimada, T. Narita, T. Kojima, K. Hirota, Application of ozone decomposition catalysts to electron-beam irradiated xylene/air mixtures for enhancing carbon dioxide production, *Radiation Physics and Chemistry* 77 (2008) 585–590.
- [278] T. Hakoda, K. Matsumoto, A. Mizuno, T. Kojima, K. Hirota, Catalytic oxidation of xylene in air using TiO<sub>2</sub> under electron beam irradiation, *Plasma Chemistry and Plasma Processing* 28 (2008) 25–37.
- [279] T. Hakoda, K. Matsumoto, A. Mizuno, T. Narita, T. Kojima, K. Hirota, Oxidation process of xylene in air using Ag/TiO<sub>2</sub> under electron beam irradiation, *IEEE Transactions on Industry Applications* 44 (2008) 1950–1956.
- [280] T. Hakoda, K. Matsumoto, A. Mizuno, K. Hirota, Oxidation of xylene and its irradiation byproducts using an electron-beam irradiating gamma-Al<sub>2</sub>O<sub>3</sub> bed, *Journal of Physics D: Applied Physics* 41 (2008).
- [281] K.P. Francke, H. Miessner, R. Rudolph, Cleaning of air streams from organic pollutants by plasma–catalytic oxidation, *Plasma Chemistry and Plasma Processing* 20 (2000) 393–403.
- [282] T. Kuroki, K. Hirai, R. Kawabata, M. Okubo, T. Yamamoto, Decomposition of adsorbed xylene on adsorbents using nonthermal plasma with gas circulation, *IEEE Transactions on Industry Applications* 46 (2010) 672–679.
- [283] S. Futamura, A.H. Zhang, H. Einaga, H. Kabashima, Involvement of catalyst materials in nonthermal plasma chemical processing of hazardous air pollutants, *Catalysis Today* 72 (2002) 259–265.
- [284] K. Krawczyk, B. Ulejczyk, Influence of water vapor on CCl<sub>4</sub> and CHCl<sub>3</sub> conversion in gliding discharge, *Plasma Chemistry and Plasma Processing* 24 (2004) 155–167.
- [285] S. Futamura, H. Einaga, A.H. Zhang, Comparison of reactor performance in the nonthermal plasma chemical processing of hazardous air pollutants, *IEEE Transactions on Industry Applications* 37 (2001) 978–985.
- [286] R. Yamashita, T. Takahashi, T. Oda, Humidity effect on non-thermal plasma processing for VOCs decomposition, in: *IAS'96—Conference Record of the 1996 IEEE Industry Applications Conference, Thirty-First IAS Annual Meeting*, vol. 1–4, 1996, pp. 1826–1829.
- [287] S. Agnihotri, M.P. Cal, J. Prien, Destruction of 1,1,1-trichloroethane using dielectric barrier discharge nonthermal plasma, *Journal of Environmental Engineering* 130 (2004) 349–355.
- [288] Y. Kim, K.T. Kim, M.S. Cha, Y.H. Song, S.J. Kim, CF<sub>4</sub> decompositions using streamer- and glow-mode in dielectric barrier discharges, *IEEE Transactions on Plasma Science* 33 (2005) 1041–1046.
- [289] S. Futamura, A.H. Zhang, T. Yamamoto, Mechanisms for formation of inorganic byproducts in plasma chemical processing of hazardous air pollutants, *IEEE Transactions on Industry Applications* 35 (1999) 760–766.
- [290] Z. Falkenstein, Effects of the O<sub>2</sub> concentration on the removal efficiency of volatile organic compounds with dielectric barrier discharges in Ar and N<sub>2</sub>, *Journal of Applied Physics* 85 (1999) 525–529.